송 재 민 교수 지도

박사학위 청구 논문

Evaluation of the recombinant protein nanoparticle based rotavirus vaccine candidate

- Establishment of evaluation method for the vaccine potency of mono and trivalent nanoparticle rotavirus vaccines -

2023

성신여자대학교 대학원

미래융용과학학과

박 영 찬

Evaluation of the recombinant protein nanoparticle based rotavirus vaccine candidate

- Establishment of evaluation method for the vaccine potency of mono and trivalent nanoparticle rotavirus vaccines -

A Dissertation Submitted to the
Graduate School of Sungshin University

in partial fulfillment of the requirements
for the degree of Doctor of Department of Next Generation Applied Sciences

Young-Chan Park

October, 2022

This is to certify that we have examined the
Doctoral Dissertation of
Young-Chan Park
Submitted to Department of Department of
Next Generation Applied Sciences

Approved as to style and content:

Thesis Advisor .....

Committee Chairman .....

Committee Member .....

Committee Member .....

Committee Member .....

Committee Member .....

The Graduate School of Sungshin University

ABSTRACT

Evaluation of the recombinant protein nanoparticle based rotavirus vaccine candidate

Young-Chan Park
Next-Generation Applied Science
Graduate School of
Sungshin University

Rotavirus A specifically is capable of infecting humans leading to intestinal disease. Each year, approximately 146,000 to 215,000 deaths caused by rotavirus infection are reported. Rotavirus A P[8] ,P[4] and P[6] serotypes are occurring worldwide. Two oral live vaccines to prevent rotavirus infection, RotaTeq® (Merck, Rahway, NJ, USA) and Rotarix® (GlaxoSmithKline, GSK, Brentford, UK) were developed and approved by the FDA. However, oral live vaccine efficiency was less than 50% in low-income countries and has side effect. VP8 protein of rotavirus A is a vaccine candidate to prevent rotavirus infection and was reported major target of neutralized antibody against rotavirus infection. However, subunit vaccine using only recombinant protein showed low immunogenic properties. To increase immunogenicity, we constructed VP8* protein to nanoparticle form by conjugation of encapsulin (ENC). P[8], P[4] and P[6]

serotypes of encapsulin conjugated VP8 (ENC-VP8*) has been confirmed to form nanoparticle using TEM and the biological function of ENC-VP8* was examined using HBGA binding assay. The monovalent or trivalent VP8* vaccine was inoculated into mice with three times to confirm the immune response. Immunization of ENC-VP8 induced binding antibody to more than immunization of P2-VP8* protein in ELISA result. Neutralized antibody titer induced by immunization of ENC-VP8* was identified through PRNT assay and HBGA blocking assay. Those result showed that ENC-VP8* forms nanoparticle and binds to HBGA. An evaluation method was established to measure antibody response and T cell response to evaluate the efficacy of rotavirus vaccine. This evaluation method compared the efficacy of encapsulin-based nanoparticle and recombinant protein-based P2-VP8* of P[8], P[4], and P[6] serotype, showing that ENC-VP8* induces highly neutralizing antibody against rotavirus infection in mice more than immunization of P2-VP8* protein. Therefore, we have shown that ENC-VP8* is an effective vaccine candidate to prevent P[8], P[4], and P[6] serotype of rotavirus infection.

Contents

List of Tables

List of Figures

Introduction

Rotavirus is classified under the family of *Reoviridea* and has a double-stranded RNA (dsRNA) genome [1]. There are a total of nine species of rotavirus, A, B, C, D, F, G, H, I, and J [2,3]. Rotavirus A specifically is capable of infecting humans leading to intestinal disease [4]. Rotavirus spreads through the fecal-oral route, damaging the small intestine and causing gastroenteritis at the age of 5 years [5,6]. Each year, approximately 146,000 to 215,000 deaths caused by rotavirus infection are reported [7,8]. Rotavirus A P[8] and P[4] serotype account for 88% of all rotavirus infections [9]. Both serotypes in addition to P[6] serotype are common worldwide [9,10]. Rotavirus infection has been reported in Korea at a rate of 66% for the P[8] serotype and 31% for the P[4] serotype, with some occurrence of the P[6] serotype rotavirus [11].

Two oral live vaccines to prevent rotavirus infection, RotaTeq® (Merck, Rahway, NJ, USA) and Rotarix® (GlaxoSmithKline, GSK, Brentford, UK), were developed and approved by the FDA [12,13]. RotaTeq® is efficacious in preventing the following types of rotaviruses: G1, G2, G3, G4 and G9 and Rotarix® is efficacious in preventing only G1 type of rotavirus [14]. Both vaccines defended against viral infections in high-income countries with high efficiency of nearly 90% [15,16]. However, in low-income and middle-income countries, vaccine efficiency was less than 50% [17]. The reasons behind the low efficiency of the vaccine in low and mid-countries are mainly differences among people' s intestinal environments [18-20]. The mechanism by which differences in intestinal environment reduce the effectiveness of oral live vaccines is the interference by intestinal

microorganisms [18-20]. Enterovirus causes intestinal dysfunction called environmental enteric dysfunction (EED) in the small intestine and appears in 80% of 12-week-old infants in the slums of underdeveloped countries [18]. These intestinal infections cause inflammatory and IgA responses that would inhibit the replication of oral live vaccines, reducing the effectiveness of vaccines [21]. Another reason is that maternal antibodies and anti-viral substances in breast milk can reduce the effectiveness of the vaccine [20]. In the case of oral live vaccines such as the live attenuated cholera vaccine and oral poliovirus vaccine, it has been reported that their efficacy is reduced due to breast milk component [22,23]. Additionally, the oral live vaccine may lead to some side effects such as diarrhea [24]. Due to the limitations of oral live vaccines, it is necessary to develop a safer and more effective vaccine to prevent the spread of the rotavirus infection [25]. To overcome the side effects and limitations of oral live vaccine, it involves a method whereby an inactivated rotavirus particle and subunit vaccine is inoculated using the intramuscularly or intradermal route [26]. Parenteral inoculation of virus antigens induces the systemic IgG and mucosal IgA response that would prevent the spread of the viral infection [26]. A parenteral subunit vaccine (P2-VP8*) was efficacious in preventing the spread of the rotavirus infection in mice experiments and clinical trials [27].

Rotavirus A consists of eight structural proteins forming three layers [28,29]. The inner layer is composed of VP2, the intermediate layer is composed of VP6, and the outer layer is composed of VP7 and VP4 [30-32]. The serotype of rotavirus A is divided according to the G serotype

antigen VP7 and the P serotype antigen VP4 [29,33]. Virus spike protein VP4 allows the rotavirus to attach to the host cell [34]. VP4 indicates virulence of the rotavirus and is cleaved into two domains, VP8 and VP5, by trypsin [6,9]. VP8 is a receptor-binding domain and VP5 allows the virus genome to enter the host cell [35]. Attachment of rotavirus to the host cell was inhibited by inducing VP8-specific antibodies suppressing an infection by rotavirus [9,35]. Among the 51 P serotypes, P[8], P[4], and P[6] occur commonly worldwide and each serotype VP8 differs structurally [9,10,29]. Effective vaccines for each of the P[8], P[4], and P[6] serotype of VP8 are needed to effectively prevent rotavirus because of the poor similarity between VP8 serotype [9,10]. VP8 is an effective vaccine candidate to prevent rotavirus infection. However, full-length VP8 is expressed as an inclusion body in *Escherichia coli* (*E. coli)* showing low immunogenicity [36]. In previous studies, modified VP8 (VP8*, 65-244aa) with N terminal truncation was prepared and expressed as a soluble form [36]. In another study, P2 T cell epitope was expressed together in VP8* (P2-G1P[8]VP8*) of G1P[8] serotype to induce VP8*-specific antibodies that will suppress a viral infection [37]. Further studies confirmed that a trivalent vaccine made by expressing VP8* with P[8], P[4], and P[6] serotypes effectively induced VP8*-specific antibody response to each serotype [38].

Other strategies for overcoming the relatively low immunogenicity of the subunit vaccine have been proposed, such as VLP and nanoparticles [39]. Nanoparticles are self-assembled protein complexes that form a spherical shape with a diameter of 30-100 nm [40]. Hepatitis B virus core protein,

VP1 of norovirus, the coat protein of MS2 bacteriophage, and bacterial encapsulin have self-assembled properties [41-44]. Nanoparticles form complexes that are easily recognized by immune cells, such as dendritic cells and macrophages, due to their similarity in size and structure to pathogens [45,46]. Dendritic cells recruit immune cells through the uptake of nanoparticles [47]. Therefore, nanoparticles can cause inflammation through interaction with recruited immune cells such as neutrophils, macrophages, and other effector cells [47]. Through this response, nanoparticles elicit an innate immune response that is more effective after vaccination [48].

Encapsulin is a bacterial cargo protein that transports ions from the inside to the outside of bacteria through the formation of capsules [49]. Encapsulin consists of 60 units of particles that are 24-32 nm in size. Encapsulin-based particles are resistant to changes in pH and temperatures [44,50]. These properties allow encapsulin to be effective in transmitting small molecular modules or displaying antigens [49,51,52]. Previous studies confirmed that the encapsulin-based nanoparticles contained various antigens such as M2e of influenza, HA system region, glycoprotein 350/220 (gp350), ovalbumin (OVA) protein, OT-1 peptide, and β-barrel of meningococcal [53-57].

In this study, nanoparticles displaying each of the VP8* serotypes, including P[8], P[4], and P[6] were created, and VP8*-specific antibody responses were measured in mice immune sera using ELISA to evaluate the efficacy of VP8* vaccines. Additionally, the ability to inhibit binding between HBGA (host cell receptor) and VP8* (rotavirus receptor-binding

domain) as well as the rotavirus neutralizing antibodies were both confirmed to evaluate the efficacy of monovalent vaccines containing P[8], P[4], and P[6] serotypes. The trivalent VP8* vaccine was immunized with mice to effectively induce an immune response for P[8], P[4], and P[6] serotypes.

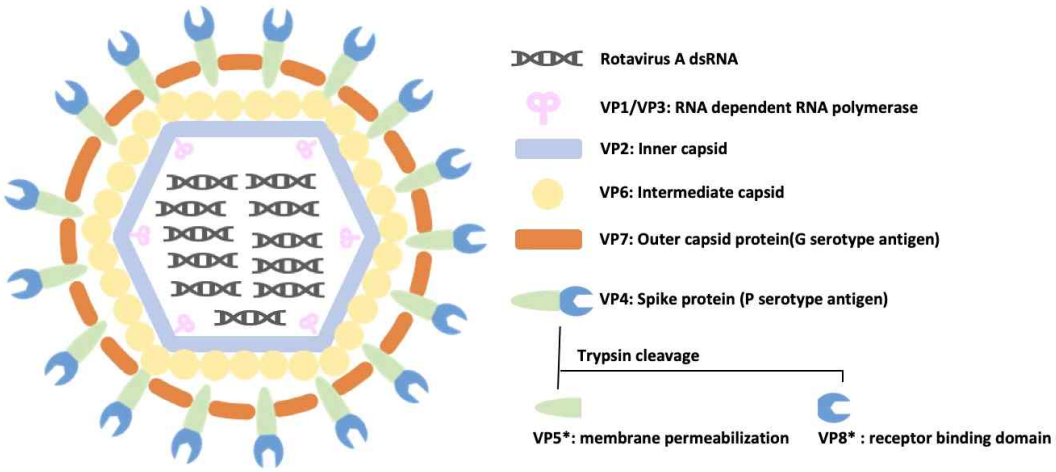

Fig 1. Structure of human rotavirus A

Rotavirus A has 11 segmented dsRNA as genomes and consists of three layers. The inner layer is composed of VP2, and inside are the dsRNA and the RNA dependent RNA polymerase (RdRp) VP1/VP3. The intermediate layer is composed of VP6. The outer layer is composed of VP7 and VP5*/VP8*, which are divided into G serotype according to VP7 and P serotype according to VP5*/VP8*.

Materials and methods

Virus and cell

A stock of MA 104 cells and rotavirus Wa (G1P[8]) strain were provided from Jeonbuk National University. The rotavirus DS-1 (G2P[4]) strain was obtained from ATCC (American Type Culture Collection, Manassas, USA) and the ST3 (G4P[6]) strain was adopted from NCPV (National Collection of Pathogenic Viruses, UK). MA 104 cells were cultured in Dulbecco's modified eagle medium (DMEM, Lonza, Basel, Switzerland) containing 10% heat-inactivated fetal bovine serum (FBS, Gibco, Billings, MT, USA) and 1% penicillin and streptomycin. The culture was incubated at 37 ℃ in a humidified air atmosphere with 5% CO_2. Three strains of rotavirus were incubated at 37 ℃ for 1 hr after 10 μg/ml of trypsin treatment. Trypsin-activated rotavirus was added to a monolayer of MA 104 cells in DMEM medium containing trypsin at a concentration of 2 μg/ml and incubated at 37 ℃ in a humidified air atmosphere with 5% CO_2 for 5 days.

Table 1. Three serotypes of rotavirus A used in this study

Serotype	Strain	Taxon ID	ATCC or NCPV no.
G1P[8]	Rotavirus A (strain RVA/Human/United States/Wa/1974/G1P1A[8])	10962	VR-2018
G2P[4]	Rotavirus A (strain RVA/Human/United States/DS-1/1976/G2P1B[4])	10950	VR-2550
G4P[6]	Rotavirus A (strain RVA/Human/United Kingdom/ST3/1975/G4P2A[6])	10960	0904053v

Expression and purification of ENC-VP8* and P2-VP8*

Encapsulin-conjugated VP8* (ENC-VP8*) vaccine and tetanus toxoid T cell epitope conjugated VP8* (P2-VP8*) were provided by Inthera Inc and expressed through *E. coli* expression system as previously described [58,59,60]. Sequence of RNA interaction domain (RID) and encapsulin were obtained in previous studies [50,61]. Encapsulin was conjugated to the VP8* sequence in strains G1P[8], G2P[4], or G2P[6] using overlapping PCR. To increase the expression efficiency of the produced ENC-VP8*, the RID was inserted into the N-terminal as a fusion partner and then cloned to the pET-9 vector as previously described [59,60,62]. Plasmids were transformed into the *E. coli* strain HMS174 (DE3) competent cells through heat shock. Colonies that accepted plasmids were screened for kanamycin and grown in Luria-Bertani (LB) broth containing 50 μg/mL of kanamycin, at 37 ℃ at 250 rpm. Recombinant proteins were induced by 0.4mM of isopropyl-β-D-thiogalactopyranoside (IPTG) overnight at 16 ℃.

Kanamycin-resistant colonies were grown until the absorbance at 600 nm reached 500 ml. Five milliliter of this culture was diluted to 1 L and grown until the optical density at 600 nm (OD600) was approximately 0.6. At this point, *E.coli.* samples were harvested from centrifugation at 4000 g during 20 min at 4 ℃. *E.coli* were lysed using a homogenizer at 1,500 bar and treated with ammonium sulfate [$(NH_4)_2SO_4$] at 1.2M end-concentrations for 30 min to precipitate RID-ENC-VP8* proteins. After centrifugation at 12,000 rpm for 10 min, the protein pellets were then dissolved in 50mM Tris buffer (pH8.0). The dissolved protein pellet was loaded into a Ni-affinity High-Performance column (200 mL bed volume, Cytiva,

Marlborough, MA, USA) followed by washing with 1% Tween 20/6M Urea to remove unbound proteins and other impurities. The bound proteins were eluted using 10 CVs of buffer B containing 300 mM imidazole in loading buffer via a linear gradient elution manner (0 to 100% buffer B). TEV protease cleavage at a ratio of 20:1 cleaved the ENC-VP8* proteins for 16 hr at 4 ℃, after which the mixture was loaded onto a second Ni-affinity High-Performance column (100 mL bed volume, Cytiva) where the target proteins that flowed through the fraction were collected. Anion exchange chromatography was performed using an AKTA Fast Performance Liquid Chromatography System (AKTA Pure 25L, GE Healthcare Life Sciences, Chicago, IL, USA) via 40 Q Work Beads (40 mL bed volume, Bio-Works) to purify the ENC-VP8* proteins. The eluted proteins were mixed with Endotoxin Removal resin (Toxin Cleanic ET Removal kit, Bioneer, Daejeon, Republic of Korea) and equilibrated with PBS. The unbound fraction containing ENC-VP8* particle was concentrated by ultrafiltration and diafiltration (UF/DF) with a 10 KDa Sartocon Slice cassette Hydrosart 0.1 m^2 (Sartorius) in formulation buffer (20 mM Tris (pH 7.5) 147 mM NaCl). The retentate was then filtered with a 0.22 μM filter (Millipore).

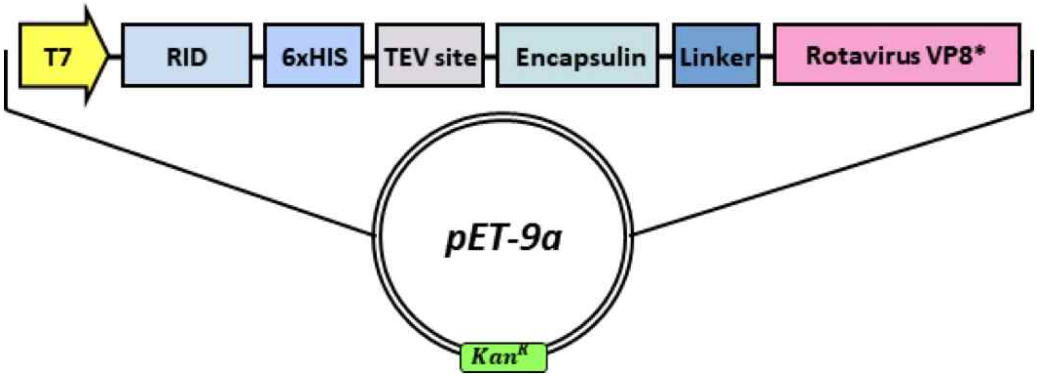

Fig 2. Vector construct for expression of encapsulin conjugated VP8* (ENC-VP8*)

RID-ENC-VP8* was transcribed under T7 promoter. N terminal has RID to increase the solubility of recombinant protein, and 6 histidine for purification using IMAC. There is a TEV cleavage site for dividing RID and ENC-VP8*. A linker was placed between encapsulin and VP8*, which was cloned with a PET-9a vector [60].

Table 2. Amino acid sequence of rotavirus VP8*

Serotype	Protein sequence	Genbank ID
G1P[8]	LDGPYQPTTFTPPTDYWILINSNTNGVVYES TNNSDFWTAVIAVEPHVNPVDRQYNVFGEN KQFNVRNDSDKWKFLEMFRGSSQNDFYNRR TLTSDTRLVGILKYGGRIWTFHGETPRATTD SSNTANLNGISITIHSEFYIIPRSQESKCNEYINN GL	FJ423116
G2P[4]	VLDGPYQPTTFKPPNDYWLLISSNTNGVVYE STNNNDFWTAVIAVEPHVSQTNRQYILFGEN KQFNVENNSDKWKFFEMFKGSSQGDFSNRR TLTSSNRLVGMLKYGGRVWTFHGETPRATT DSSNTADLNNISIIIHSEFYIIPRSQESKCNEYIN NGL	M88480
G2P[6]	VLDGPYQPTSFKPPSDYWILLNPTNQQVVLE GTNKTDIWVALLLVEPNVTNQSRQYTLFGET KQITVENNTNKWKFFEMFRSSVSAEFQHKRT LTSDTKLAGFLKFYNSVWTFYGETPHATTD YSSTSNLSEVETAIHVEFYIIPRSQESKCNEYIN TGL	EF672577

Table 3. Amino acid sequence of encapsulin

Organism	Protein sequence	Protein ID
Thermotoga maritima MSB8	MEFLKRSFAPLTEKQWQEIDNRAREI FKTQLYGRKFVDVEGPYGWEYAAHP LGEVEVLSDENEVVKWGLRKSLPLIE LRATFTLDLWELDNLERGKPNVDLSS LEETVRKVAEFEDEVIFRGCEKSGVK GLLSFEERKIECGSTPKDLLEAIVRALS IFSKDGIEGPYTLVINTDRWINFLKEE AGHYPLEKRVEECLRGGKIITTPRIED ALVVSERGGDFKLILGQDLSIGYEDRE KDAVRLFITETFTFQVVNPEALILLKF	WP_004080898.1

Characterization of ENC VP8* and P2-VP8*

Characterization of ENC-VP8* and P2-VP8* were done by Inthera Inc. Sodium dodecyl sulfate-polyacrylamide gel electrophoresis (SDS-PAGE) was utilized to determine the purity and identify the target protein and cleaved ENC-VP8*. ENC-VP8* and P2-VP8* were separated by 12% polyacrylamide gel and stained using coomassie blue stain solution.

Morphology of ENC-VP8* was confirmed under transmission electron microscopy (TEM). The grid was negatively stained with 2% uranyl acetate, dried, examined, and randomly captured. ENC-G1P[8]VP8*, ENC-G2P[4]VP8*, and ENC-G2P[6]VP8* were examined using a Talos L120C transmission electron microscope (FEI, Czech) at an accelerating voltage of 120 kV. Formvar/carbon-coated TEM grid (EMS).

Binding of ENC-VP8* and P2-VP8* to synthesized oligosaccharides

Histo-blood group antigens (HBGAs) binding assays were used to confirm the binding of ENC-VP8* and P2-VP8* to synthesized oligosaccharides as previously described [63]. Briefly, we used five biotin-conjugated HBGAs which are Lea, Led H Type 1, and H type 2. One microgram of biotin-conjugated HBGAs was added to Neutravidin-coated, 96-well microtiter plates (Pierce Thermofisher Scientific, Rockford, IL, USA) and incubated at room temperature (RT) for 5 hr. Then, three serotypes of ENC-VP8* or P2-VP8* were added and incubated at 4 ℃ overnight. To detect the proteins attached to HBGA, G1P[8]VP8*, G2P[4]VP8*, or G2P[6]VP8* immunized mice sera were added and incubated at RT for 1

hr. Horseradish peroxidase (HRP)-conjugated goat anti-mouse IgG (Southern Biotech) was added at 1:5000 as the secondary antibody and incubated at RT for 1 hr, after which the substrate of the TMB solution was added and incubated for 10 min. The reaction was stopped by adding 50 μl/well of 0.5M sulfuric acid. The reaction signals were measured at 450 nm.

Vaccine formulation and mice immunization

For the animal experiment, female BALB/C mice 4 weeks of age were immunized by intramuscular administration. A monovalent G1P[8] VP8* vaccine was inoculated with 1 μg (Low), 5 μg (Mid), or 10 μg (High) of ENC-G1P[8]VP8* or 10 μg (High) of P2-G1P[8]VP8* in a group of mice (n=6). A monovalent G2P[4] VP8* or G2P[6] VP8* vaccine was inoculated into 6 mice, each with 0.5 μg (Low), 2 μg (Mid), or 8 μg (High) of ENC-VP8* or 8 μg (High) of P2-VP8*. A trivalent VP8* vaccine was inoculated into 6 mice with 1.5 μg (Low), 6 μg (Mid), or 24 μg (High) of ENC-VP8* (each with the same amount of serotype ENC-VP8*) or 24 μg (High) of P2-VP8* (each with the same amount of serotype P2-VP8*). All proteins were diluted with a PBS buffer and prepared by mixing with aluminum hydroxide (Alhydrogel, cat# vac-alu-250, InvivoGen, San Diego, CA, USA) at a 1:1 ratio as previously described [38]. The mice received the vaccination 3 times at 2 weeks intervals. After 2 weeks of vaccination, a serum sample was obtained through retro-orbital bleeding. After a final inoculation, feces were collected and resuspended into a PBS buffer at 3, 7, and 14 days. All animal experiments and protocols were approved by the Institutional Animal Care and Use Committee (IACUC) of the Sungshin Women's University (Assurance no. SSWIACUC-2021-007).

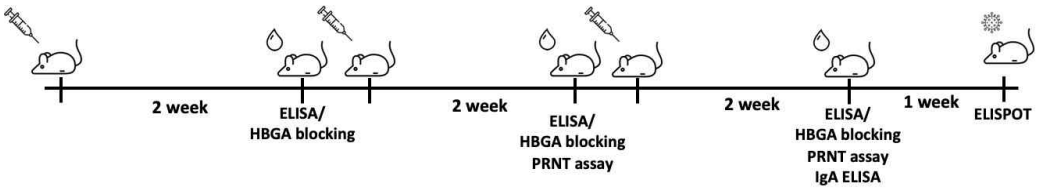

Fig 3. Schedule of mice experiment.

BALB/C mice were inoculated with VP8* vaccine into intramuscular administration and received 3 times at interval of 2 weeks. After 2 week of vaccination, serum sample were obtained by retro-orbital bleeding. Post 3 week final vaccination, mice were infected with 100 PFU of rotavirus Wa (G1P[8]), DS-1 (G2P[4]) or ST3 (G4P[6]) strain in PBS buffer and inoculated into intranasally administration.

Determination of antigen-specific antibody responses

Rotavirus specific antibody responses were detected using an ELISA assay as previously described [64]. Briefly, plates were coated with 100 μl containing 10 ng of P2-G1P[8]VP8*, m P2-G1P[6]VP8*, and P2-G2P[6]VP8* at 4 ℃ overnight. Plates were incubated with 3% BSA solution at 37 ℃ for 1.5 hr and 100 μl of diluted serum or feces sample was added and incubated again at 37 ℃ for 1.5 hr. For determination of serum IgG or IgA response, a PBS buffer containing 1:1000-1:2000 diluted goat anti-mouse IgG HRP or goat anti-mouse IgA HRP was added and incubated at 37 ℃ for 1 hr. The TMB solution substrate was added and incubated for 10 min. The reaction was stopped by adding 50 μl/well of 0.5M sulfuric acid. The reaction signals were measured at 450 nm.

Antibody response inhibiting the binding with synthesized oligosaccharides

Antibody reactions that inhibit binding between Led H type 1 and ENC VP8 in serum were measured as previously described [65]. Briefly, 1 μg of biotin-conjugated Led H type 1 was added to Neutravidin-coated 96-well microtiter plates (Pierce Thermofisher Scientific, Rockford, IL, USA) and incubated at RT for 5 hr. At the same time, G1P[8], G2P[4], or G2P[6] ENC-VP8* at a concentration of 2 μg/ml and a serially diluted serum were mixed and reacted at 37 ℃ for 3 hr. Serum-VLP solution was added to a plate and incubated at 4 ℃ overnight. To detect whether ENC-VP8* was attached to HBGA, rotavirus-specific rabbit polyclonal antibodies were added at 1:500 dilution and incubated at RT for 1 hr. HRP-conjugated goat

anti-rabbit IgG (Invitrogen, Waltham, MA, USA) was added at 1:5000 as a secondary antibody and incubated at RT for 1 hr. The TMB solution substrate was added and incubated for 10 min. Finally, the reaction was stopped by adding 50 μl/well of 0.5M sulfuric acid. The reaction signals were measured at 450 nm and the blocking index was calculated using the following formula.

$$Bloking\ \ Index = \frac{(VLP\,only - background) - (VLP with\ serum - background)}{(VLP\,only - background)}$$

Plaque reduced neutralization antibody response

Neutralizing antibodies that inhibit rotavirus infection were identified through previously described methods [66]. Briefly, MA-104 cells were added to a 6-well plate with $5x10^6$ cells per well. On the following day, 100 PFU of infectious rotavirus Wa (G1P[8]), DS-1 (G2P[4]), or ST3 (G4P[6]) strain were treated with trypsin at a concentration of 10 μg/ml and incubated at 37 ℃ for 1 hr. The serum was diluted two folds serially after heat treatment at 56 ℃ for 30 min. Trypsin-activated rotavirus was incubated at 37 ℃ for 1 hr with serially diluted heat-inactivated serum. The virus-serum solution containing 2 μg/ml concentrations of trypsin was added to a monolayer of MA-104 cells and shaken at 15 min intervals and incubated at 37 ℃ for 1 hr. After 1 hour, the inoculums were removed and the overlay media containing trypsin at a concentration of 2 μg/ml was made by mixing 1.4% agarose and 2 x DMEM media in a 1:1 ratio. The mixture was added to a 6-well plate and incubated at 37 ℃ in a humidified air atmosphere with 5% CO2 for 5 days, after which the plaques were counted for the 50% plaque reduction neutralization test

($PRNT_{50}$) calculation.

Virus-specific T-cell response

Vaccination of ENC VP8 induced a T-cell response that was detected by the ELISPOT assay as previously described [67]. After 3 weeks of vaccinations, the mice were infected with 100 PFU of the rotavirus Wa (G1P[8]), DS-1 (G2P[4]), or ST3 (G4P[6]) strain in PBS buffer and inoculated through intranasal administration. Multiscreen 96-well filtration plates (Millipore) were coated with anti-mouse interferon-gamma (IFN-γ) or anti-mouse interleukin-4 (IL-4) at a concentration of 3 μg/ml at 4 ℃ overnight and filled with an RPMI medium containing 10% FBS. Freshly isolated splenocytes ($1x10^6$cell) were added into IL-4 and IFN-γ specific antibody-coated plates, mixed with 1 μg/ml of inactivated rotavirus Wa (G1P[8]), DS-1 (G2P[4]), or ST3 (G4P[6]) solution, and incubated at 37 ℃ with 5% CO_2 for 40 hr. Biotin-conjugated anti-IL-4 & anti-IFN-γ were then added and incubated at 4 ℃ overnight, after which streptavidin-HRP was added and incubated for 1.5 hr at RT. DAB solution was added to develop spots that were counted using an ELISPOT reader.

Result

Characterization of ENC-VP8* and P2-VP8*

G1P[8], G2P[4], and G2P[6] serotypes of ENC-VP8* and P2-VP8* were expressed using *E. coli*, and SDS PAGE and TEM results were provided by Inthera Inc. The expression of each purified ENC-VP8* in *E.coli* was confirmed by SDS PAGE. After immobilized metal ion affinity chromatography (IMAC) purification, RID-ENC-VP8* G1P[8], G2P[4], and G2P[6] serotypes were all expressed as approximately 70 kDa (Fig. 4). After removing the RID with TEV, the three serotypes of ENC-VP8* appeared to be approximately 53 kDa in size (Fig. 4). RID and TEV were removed using IMAC and confirmed with SDS PAGE. After the endotoxin was removed and purified through ion exchange chromatography (IEX), G1P[8], G2P[4], and G2P[6] serotypes of ENC-VP8* were identified to have a size of approximately 53 kDa (Fig. 4). The size of P2-VP8* for all three serotypes was also confirmed through SDS-PAGE to be approximately 18Kda (Fig. 5). The morphology of ENC-VP8* was observed through a transmission electron microscope, and all three serotypes of ENC-VP8* formed nanoparticles with a size of approximately 24 nm (Fig. 6). The binding ability between the VP8* vaccine and the three HBGAs (Led H type 1, Lea, and H type 2) was measured using the HBGA binding assay. G1P[8], G2P[4], and G2P[6] serotype of VP8* showed the strongest binding response to Led H type 1, followed by Lea, and H type 2. Additionally, ENC-VP8* was measured to be more tightly bound to HBGA than P2-VP8*. (Fig. 6).

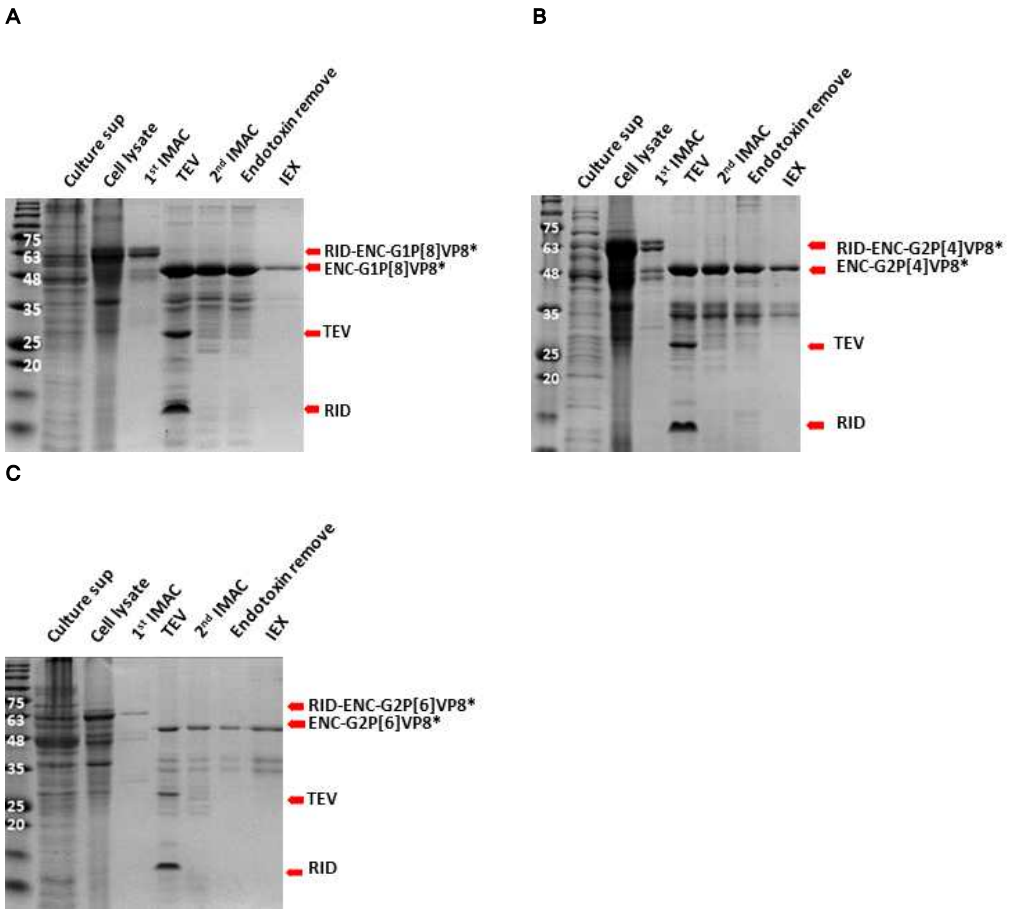

Fig 4. SDS PAGE analysis of ENC-VP8*

SDS-PAGE analysis of protein expression and purification of ENC-G1P[8]VP8* (A), ENC-G2P[4]VP8* (B) and ENC-G2P[6]VP8* (C). Lane 1. Molecular size marker. Lane 2. Culture supernatant. Lane 3. cell lysate. Lane 4. 1st IMAC elution. Lane 5. TEV protease treatment. Lane 6. 2nd IMAC flow through. Lane 7. Endotoxin removal resin. Lane 8. IEX chromatography elution [60].

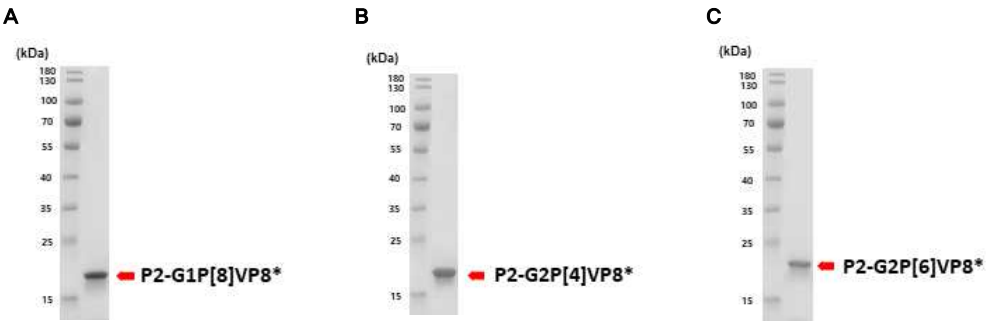

Fig 5. SDS PAGE analysis of P2-VP8*

SDS PAGE analysis of soluble P2-VP8* expressed in *E.coli*. Lane 1. molecular size marker. Lane 2. P2-G1P[8]VP8* (A), P2-G2P[4]VP8* (B) and P2-G2P[6]VP8* (C) [60].

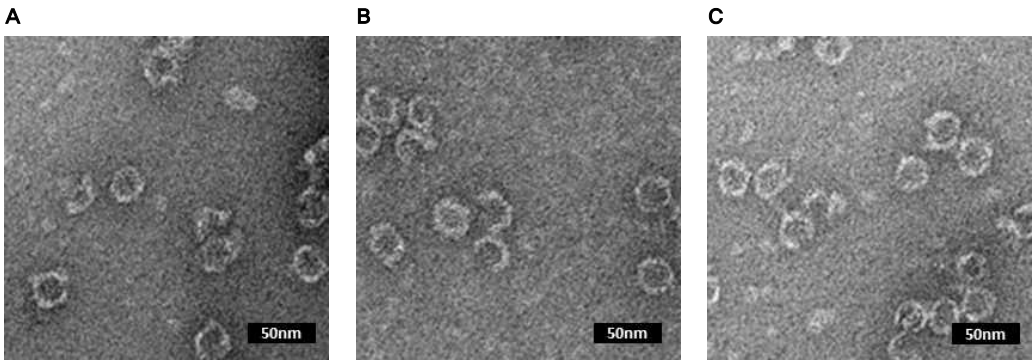

Fig 6. Morphological analysis of ENC-VP8* under transmission electron microscopy.

Morphological analysis of ENC-VP8* under transmission electron microscopy. ENC-G1P[8]VP8* (A), ENC-G2P[4]VP8* (B) and ENC-G2P[6]VP8* (C) were negatively stained with 2% uranyl acetate. Particle morphology were examined by using Talos L120C Transmission electron microscope (FEI, Czech) at an accelerating voltage of 120 kV [60].

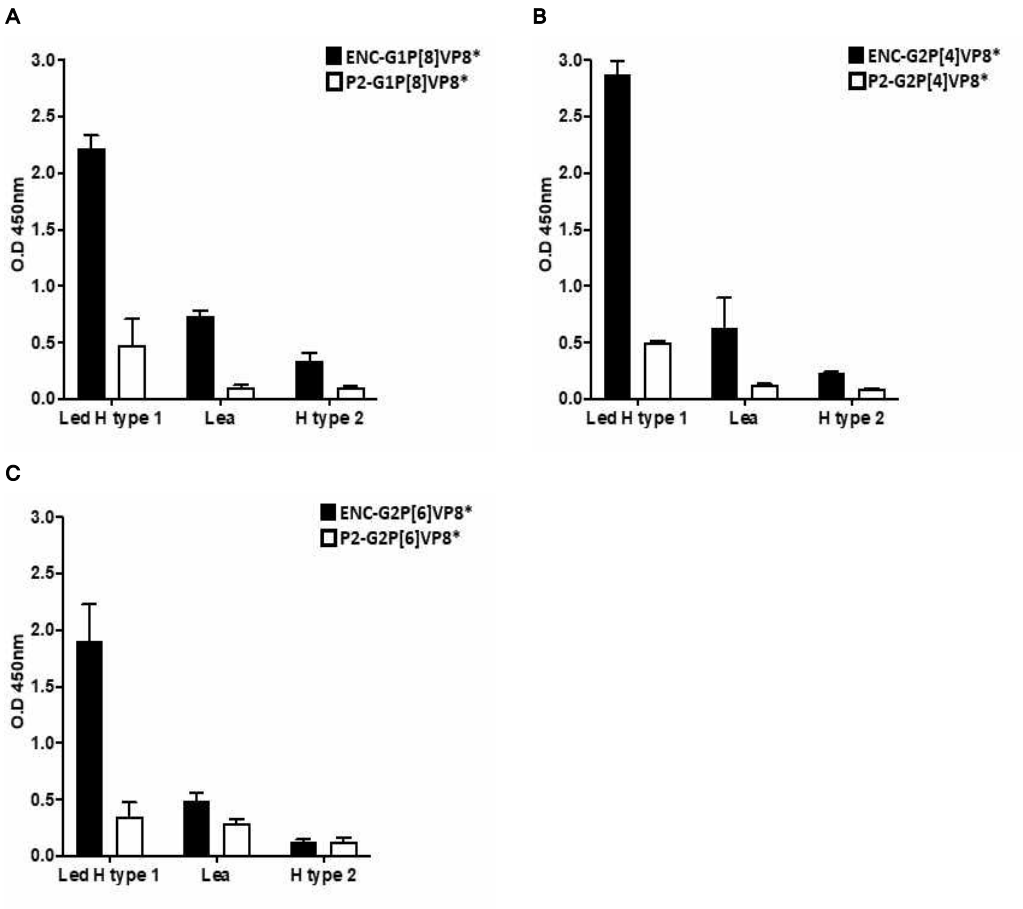

Fig 7. HBGA binding analysis of ENC-VP8* and P2-VP8*

HBGA binding assay of G1P[8]VP8* (A), G2P[4]VP8* (B) and G2P[6]VP8* (C). Three HBGA were coated at 10 μg/mL concentration. ENC-VP8* and P2-VP8* were added at a concentration of 2 μg/mL.

VP8* specific antibodies response of the monovalent vaccine

The response to IgG and IgA specific to VP8* (receptor binding domain of spike protein VP4) induced by monovalent VP8* vaccine inoculation in mice was measured using ELISA. Two weeks after vaccination, the IgG responses were measured in an immunized serum. After the last vaccine, feces samples were obtained after 3, 7, and 14 days to measure the IgA response. For G1P[8], VP8* monovalent vaccine, a high-dose of ENC-G1P[8]VP8* induced the highest G1P[8] VP8*-specific antibody response in a prime immunized pooling serum (approximately 10-fold higher than the high dose P2-G1P[8]VP8*) (Table 4). After a boost vaccination, a high dose of ENC-G1P[8]VP8* increased antibody response by about 100-folds. A mid dose and low dose of ENC-G1P[8]VP8* increased antibody response by approximately 30-fold, and P2-G1P[8]VP8* increased antibody response by about 20-folds (Table 4). After the final vaccination, the antibody response increased more compared to the boost vaccination, and the low dose of ENC-G1P[8]VP8* showed a higher antibody response than the high-dose P2-G1P[8]VP8* (Table 4). The antibody response was measured in diluted individual sera of G1P[8]VP8* monovalent vaccine immunized mice and only the high-dose of ENC-G1P[8]VP8* showed a statistically significant increase in antibody response after prime vaccination (Fig. 8A). After the boost vaccination, both ENC-G1P[8]VP8* and P2-G1P[8]VP8* exhibited G1P[8]VP8*-specific IgG responses, and all ENC-G1P[8]VP8* immunized groups induced higher antibody responses than P2-G1P[8]VP8* immunization with statistical significance (Fig. 8B). After the final vaccination, mid and high doses of

ENC-G1P[8]VP8* induced a higher antibody response than P2-G1P[8]VP8*, and a low dose of ENC-G1P[8]VP8* induced a higher antibody response than P2-G1P[8]VP8*, but showed no statistically significant difference (Fig. 8C) Three days after the final vaccination, ENC-G1P[8]VP8* showed higher IgA response than P2-G1P[8]VP8*, but showed similar response after 7 days (Fig. 9).

After the prime vaccination of the G2P[4]VP8* monovalent vaccine, G2P[4]VP8*-specific IgG response was induced in the pooled mid and high-dose of ENC-G2P[4]VP8* immunized serum (Table 5). After the boost vaccination, inoculation of both ENC-G2P[4]VP8* and P2-G2P[4]VP8* showed G2P[4]VP8* specific IgG responses, whereby ENC-G2P[4]VP8* immunized mice was induced a higher IgG response than P2-G2P[4]VP8* immunized mice (Table 5). Even after the final vaccination, the IgG response was increased compared to the boost vaccination. The IgG response from the high dose of ENC-G2P[4]VP8* was more than 5-fold greater than that of P2-G2P[4]VP8 (Table 5). The immune sera were diluted to 1:5000 to measure G2P[4]VP8*-specific antibody responses for each mouse, and only ENC-G2P[4]VP8* showed statistically significant IgG responses after prime vaccination (Fig. 10A). After the boost vaccination, three ENC-G2P[4]VP8* immunization groups had a statistically significantly higher IgG response than P2-G2P[4]VP8* and only mid and high doses of ENC-G2P[4]VP8* showed a higher statistically significant IgG response after the final inoculation (Fig. 10B and C). Low-dose ENC-G2P[4]VP8* induced a higher IgG response than P2-G2P[4]VP8* that was not statistically significant (Fig. 10C). The induced G2P[4]VP8* specific IgA response

measured in mouse feces after 3 days of final vaccination showed the highest levels of ENC-G2P[4]VP8*. After 7 days, levels of ENC-G2P[4]VP8* and P2-G2P[4]VP8* were similar (Fig. 11).

In the pooling sera with a prime G2P[6] VP8* monovalent vaccine, the IgG response was the highest in ENC-G2P[6]VP8*. Mid and high doses of ENC-G2P[6]VP8* induced a higher antibody response than P2-G2P[6]VP8* (Table 6). In the boost and final vaccinations, IgG response increased with the number of vaccinations. The IgG response in P2-G2P[6]VP8* was higher than low-dose ENC-G2P[6]VP8*, but still lower than mid and high-doses of ENC-G2P[6]VP8* (Table 6). Mice sera inoculated with G2P[6]VP8* monovalent vaccine showed statistically significant IgG responses compared to negative controls in prime vaccination (Fig. 12A). In the boost vaccination, mid and high-doses of ENC-G2P[6]VP8* induced statistically significantly higher IgG responses than P2-G2P[6]VP8*, while low doses of ENC-G2P[6]VP8* showed no statistically significant IgG response (Fig. 12B). After the final vaccination, IgG responses of high doses of ENC-G2P[6]VP8* induced a statistically significant level higher than P2-G2P[6]VP8* and mid-dose ENC-G2P[6]VP8* induced a high-level IgG response that showed no statistically significant difference (Fig. 12C). The IgA response was seen in feces samples after the final vaccination, whereby the response from ENC-G2P[6]VP8* was slightly higher than P2-G2P[6]VP8* (Fig. 13). There results confirmed that ENC-VP8* induces higher IgG and IgA reactions than P2-VP8* for G1P[8], G2P[4] and G2P[6] monovalent vaccines.

Table 4. G1P[8]VP8* specific IgG response of G1P[8]VP8* monovalent vaccine immunized sera

Group	Endpoint dilution titer		
	Prime	Boost	2^{nd} Boost
Mock	N.D	N.D	N.D
P2-VP8*(G1P[8]) High	$1.03x10^3 \pm 0.12$	$0.22x10^5 \pm 0.12$	$0.85x10^6 \pm 0.04$
ENC-VP8*(G1P[8]) Low	$1.41x10^3 \pm 0.11$	$0.39x10^5 \pm 0.11$	$1.79x10^6 \pm 0.12$
ENC-VP8*(G1P[8]) Mid	$7.72x10^3 \pm 0.04$	$2.03x10^5 \pm 0.10$	$6.83x10^6 \pm 0.19$
ENC-VP8*(G1P[8]) High	$1.02x10^4 \pm 0.09$	$1.73x10^6 \pm 0.09$	$7.02x10^6 \pm 0.03$

Cut off value was calculated as mean of negative serum at dilution 1:1000 + 3 x standard error

N.D had end point titer of less than 1000

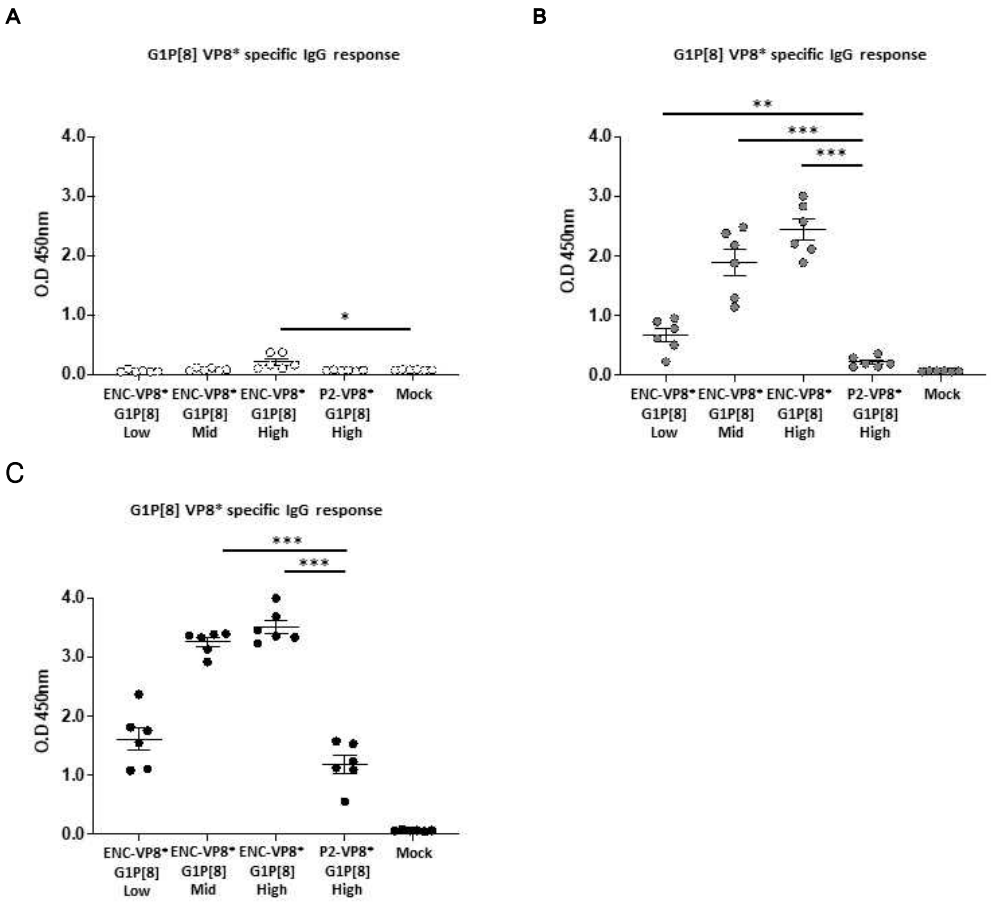

Fig 8. G1P[8]VP8* specific IgG response of G1P[8]VP8* monovalent vaccine immunized individual mice sera

G1P[8]VP8* specific antibody responses in mice immune serum. BALB/C mice were immunized 3 times with P2-G1P[8]VP8* or ENC-G1P[8]VP8*. Immune serum were diluted at 1:5000 ratio and added to recombinant protein VP8* coated plate. VP8* antigen specific IgG were determined in prime (A), Boost (B) and 2nd boost (C) immune serum. Statistically significant differences were further analyzed using T test. $*P < 0.05$ $**P < 0.01$ and $***P < 0.005$.

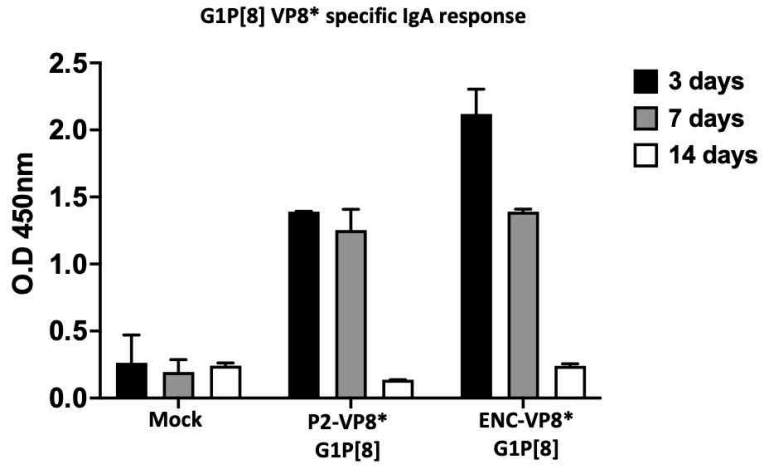

Fig. 9. G1P[8]VP8* specific IgA response of G1P[8]VP8* monovalent vaccine

G1P[8]VP8* specific IgA responses in fecal extracts. Feces were collected from immunized mice in 3, 7 and 14 days after final immunization respectively. Levels of IgA in the feces were determined by ELISA.

Table 5. G2P[4]VP8* specific IgG response of G2P[4]VP8* monovalent vaccine immunized sera

Group	Endpoint dilution titer		
	Prime	Boost	2^{nd} Boost
Mock	N.D	N.D	N.D
P2-VP8*(G2P[4]) High	N.D	$0.12x10^5 \pm 0.01$	$0.55x10^6 \pm 0.04$
ENC-VP8*(G2P[4]) Low	N.D	$2.21x10^5 \pm 0.02$	$0.67x10^6 \pm 0.02$
ENC-VP8*(G2P[4]) Mid	$2.40x10^3 \pm 0.06$	$2.48x10^5 \pm 0.02$	$0.87x10^6 \pm 0.01$
ENC-VP8*(G2P[4]) High	$1.52x10^4 \pm 0.05$	$5.36x10^5 \pm 0.49$	$2.91x10^6 \pm 0.06$

Cut off value was calculated as mean of negative serum at dilution 1:1000 + 3 x standard error

N.D had end point titer of less than 1000

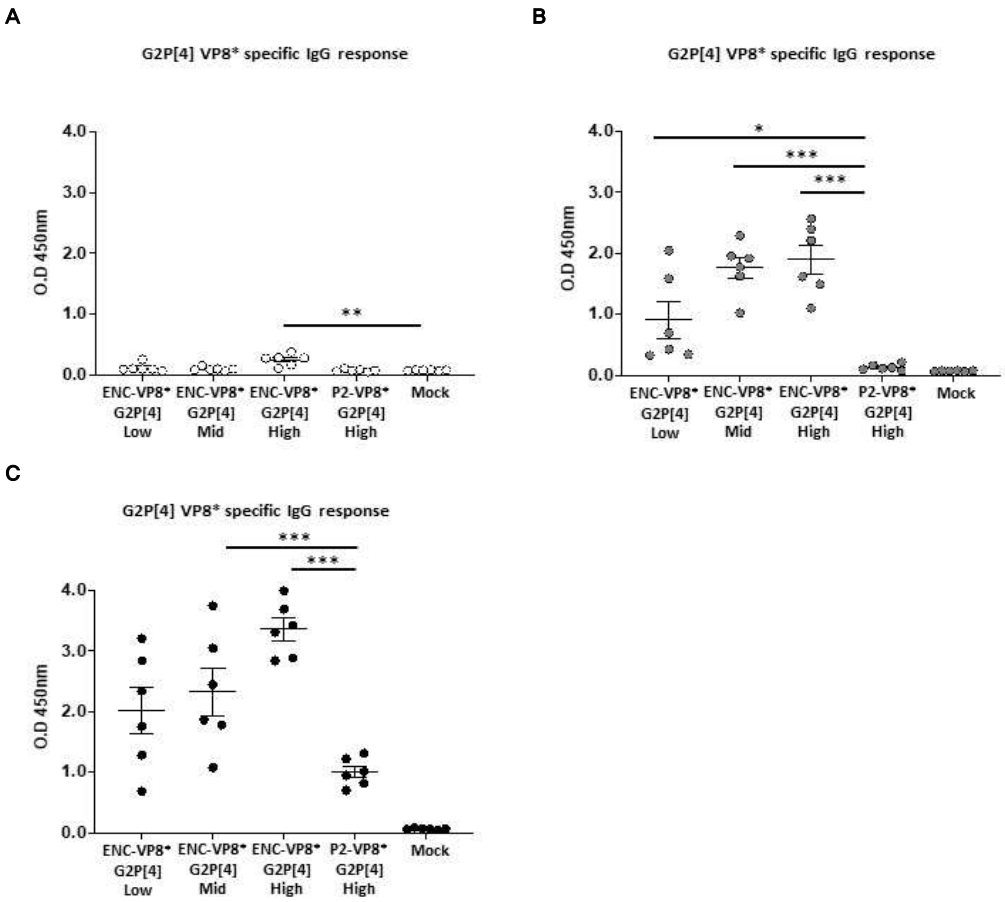

Fig 10. G2P[4]VP8* specific IgG response of G2P[4]VP8* monovalent vaccine immunized individual mice sera

G2P[4]VP8* specific antibody responses in mice immune serum. BALB/C mice were immunized 3 times with P2-G2P[4]VP8* or ENC-G2P[4]VP8*. Immune serum were diluted at 1:5000 ratio and added to recombinant protein VP8* coated plate. VP8* antigen specific IgG were determined in prime (A), Boost (B) and 2nd boost (C) immune serum. Statistically significant differences were further analyzed using T test. $*P < 0.05$ $**P < 0.01$ and $***P < 0.005$.

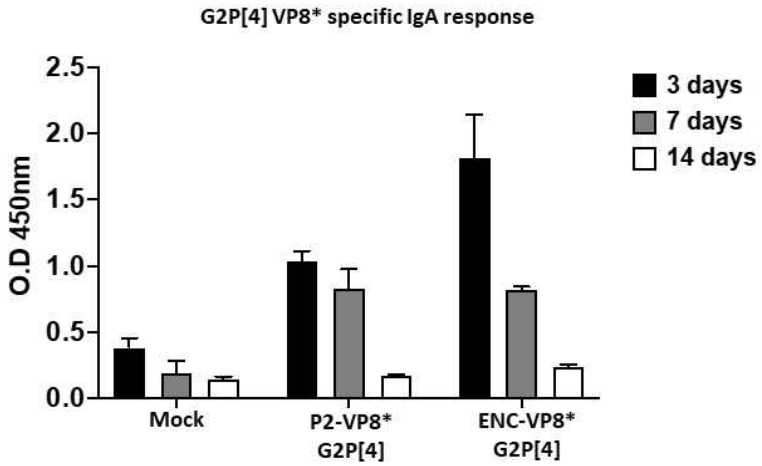

Fig. 11. G2P[4]VP8* specific IgA response of G2P[4]VP8* monovalent vaccine

G2P[4]VP8* specific IgA responses in fecal extracts. Feces were collected from immunized mice in 3, 7 and 14 days after final immunization respectively. Levels of IgA in the feces were determined by ELISA.

Table 6. G2P[6]VP8* specific IgG response of G2P[6]VP8* monovalent vaccine immunized sera

Group	Endpoint dilution titer		
	Prime	Boost	2nd Boost
Mock	N.D	N.D	N.D
P2-VP8*(G2P[6]) High	$2.90x10^4 \pm 0.22$	$1.06x10^5 \pm 0.11$	$0.83x10^6 \pm 0.04$
ENC-VP8*(G2P[6]) Low	$2.28x10^4 \pm 0.15$	$0.52x10^5 \pm 0.01$	$0.23x10^6 \pm 0.02$
ENC-VP8*(G2P[6]) Mid	$3.76x10^4 \pm 0.23$	$1.13x10^6 \pm 0.04$	$1.10x10^6 \pm 0.07$
ENC-VP8*(G2P[6]) High	$5.31x10^4 \pm 0.07$	$1.07x10^6 \pm 0.03$	$2.01x10^6 \pm 0.01$

Cut off value was calculated as mean of negative serum at dilution 1:1000 + 3 x standard error

N.D had end point titer of less than 1000

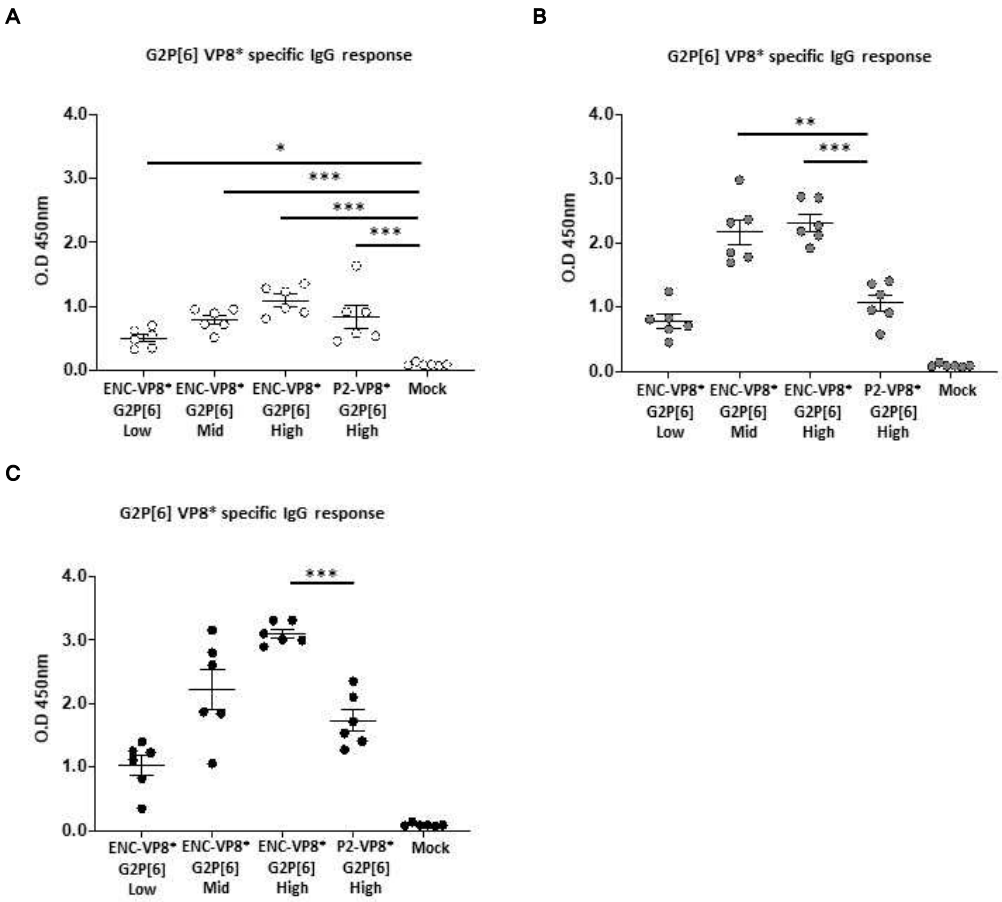

Fig 12. G2P[6]VP8* specific IgG response of G2P[6]VP8* monovalent vaccine immunized individual mice sera

G2P[4]VP8* specific antibody responses in mice immune serum. BALB/C mice were immunized 3 times with P2-G2P[4]VP8* or ENC-G2P[4]VP8*. Immune serum were diluted at 1:5000 ratio and added to recombinant protein VP8* coated plate. VP8* antigen specific IgG were determined in prime (A), Boost (B) and 2nd boost (C) immune serum. Statistically significant differences were further analyzed using T test. $*P < 0.05$ $**P < 0.01$ and $***P < 0.005$.

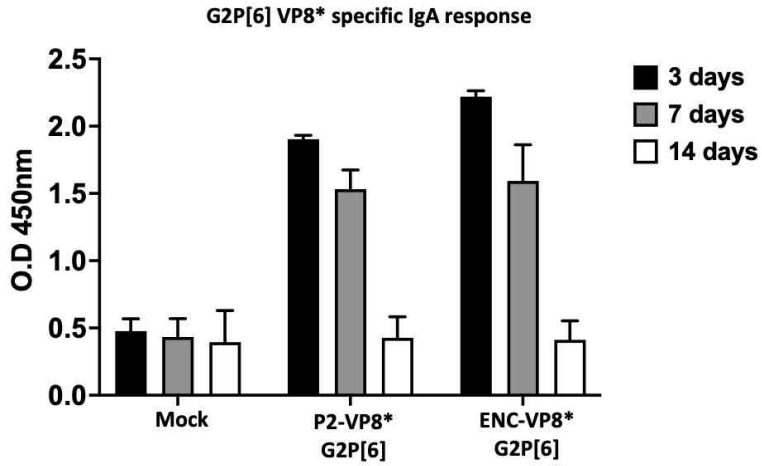

Fig. 13. G2P[6]VP8* specific IgA response of G2P[6]VP8* monovalent vaccine

G2P[6]VP8* specific IgA responses in fecal extracts. Feces were collected from immunized mice in 3, 7 and 14 days after final immunization respectively. Levels of IgA in the feces were determined by ELISA.

VP8* specific antibodies response of the trivalent vaccine

Using the ELISA assay, 14 days after vaccination, inoculation in mice in the pooling sera confirmed the VP8* specific IgG response induced by G1P[8], G2P[4], and G2P[6] trivalent VP8* vaccine. In the prime serum, G1P[8]VP8* specific IgG responses were induced only in mid and high doses of trivalent ENC-VP8*, and G2P[4]VP8*. G2P[6]VP8* specific IgG responses were induced in all groups (Table 7). High-dose trivalent ENC-VP8* induced the highest IgG response for all three serotypes of VP8* (Table 7). In the boost vaccination, the G1P[8]VP8*-specific IgG response was measured to be approximately 2-folds higher in a mid dose of trivalent ENC-VP8* and approximately 7-folds higher in high doses of trivalent ENC-VP8* compared to trivalent P2-VP8* (Table 7). The G2P[4] VP8* specific IgG response in mid and high doses of trivalent ENC-VP8* was shown to be more than 10-fold higher than trivalent P2-VP8* (Table 7). The G2P[6] VP8* specific IgG response in a mid dose of trivalent ENC-VP8* was shown to be more than 4-folds higher than that of trivalent P2-VP8* (Table 7). Even after the final vaccination, mid and high doses of trivalent ENC-VP8* induced higher antibody response than trivalent P2-VP8* and increased IgG response compared to the boost vaccination.

Serum was diluted at a ratio of 1:5000 for each mouse to measure specific IgG responses for VP8*, G1P[8], G2P[4], and G2P[6] serotypes. Only high doses of trivalent ENC-VP8* induced G1P[8] VP8*-specific IgG response with a statistically significant level in prime vaccination (Fig. 14A). In the immune serum after boost vaccination, mid and high doses of

trivalent ENC-VP8* showed higher IgG response than trivalent P2-VP8* and low doses of trivalent ENC-VP8* induced similar levels to trivalent P2-VP8* (Fig. 14B). Similarly, after the final vaccination, mid and high doses of trivalent ENC-VP8* induced a statistically significant level of IgG response higher than that in trivalent P2-VP8* (Fig. 14C). The G2P[4]VP8* specific IgG response was statistically significant in the three trivalent ENC-VP8* immunization groups in the prime vaccination (Fig. 14D). After the boost vaccination, mid and high doses of trivalent ENC-VP8* induced a higher IgG response than trivalent P2-VP8*, and low doses of trivalent ENC-VP8* showed lower levels than trivalent P2-VP8*, however with no statistically significant difference (Fig. 14E). After the final vaccination, G2P[4] VP8* specific IgG response of high dose trivalent ENC-VP8* immunization was higher than trivalent P2-VP8* with statistical significance, and a mid-dose trivalent ENC-VP8* induced a slightly higher G2P[4] VP8* specific IgG response than trivalent P2-VP8*, however, with no statistically significant difference (Fig. 14F). In prime vaccinations, the G2P[6] VP8* specific IgG response was statistically significant in all trivalent vaccine immunized mice (Fig. 14G). Following the boost vaccination, mid and high doses of trivalent ENC-VP8* induced a higher G2P[6] VP8* specific IgG response than that of trivalent P2-VP8*, similar to G1P[8] and G2P[4] VP8* specific IgG response (Fig. 14H). After the final vaccination, only a high dose of trivalent ENC-VP8* was higher than that of trivalent P2-VP8* with statistical significance (Fig. 14F). Three days after the final inoculation, measured IgA responses in feces showed that trivalent ENC-VP8* was slightly higher than trivalent P2-VP8*. On day 7,

the levels of trivalent ENC-VP8* and P2-VP8* were reduced to a similar level (Fig. 15). As a result, it was found that the trivalent ENC-VP8* inoculation induced a higher G1P[8], G2P[4] and G2P[6] specific antibody response than the trivalent P2-VP8*.

Table 7. VP8* specific IgG response of the trivalent vaccine immunized sera

Coating antigen	Group	Endpoint dilution titer		
		Prime	Boost	2nd Boost
G1P[8] VP8*	Mock	N.D	N.D	N.D
	P2-VP8* Trivalent High	N.D	$1.23x10^5 \pm 0.45$	$2.61x10^5 \pm 0.04$
	ENC-VP8* Trivalent Low	N.D	$0.68x10^5 \pm 0.09$	$2.11x10^5 \pm 0.05$
	ENC-VP8* Trivalent Mid	$3.18x10^3 \pm 0.13$	$2.72x10^5 \pm 0.06$	$3.39x10^6 \pm 0.06$
	ENC-VP8* Trivalent High	$3.52x10^3 \pm 0.11$	$8.93x10^5 \pm 0.05$	$4.49x10^6 \pm 0.03$
G2P[4] VP8*	Mock	N.D	N.D	N.D
	P2-VP8* Trivalent High	$3.51x10^3 \pm 0.25$	$0.78x10^5 \pm 0.04$	$2.61x10^6 \pm 0.09$
	ENC-VP8* Trivalent Low	$1.41x10^3 \pm 0.31$	$0.65x10^5 \pm 0.02$	$2.25x10^6 \pm 0.06$
	ENC-VP8* Trivalent Mid	$3.52x10^3 \pm 0.04$	$9.41x10^5 \pm 0.09$	$3.25x10^6 \pm 0.24$
	ENC-VP8* Trivalent High	$4.12x10^3 \pm 0.08$	$1.14x10^6 \pm 0.15$	$4.83x10^6 \pm 0.05$
G2P[6] VP8*	Mock	N.D	N.D	N.D
	P2-VP8* Trivalent High	$1.51x10^4 \pm 0.01$	$2.38x10^5 \pm 0.12$	$0.73x10^6 \pm 0.02$
	ENC-VP8* Trivalent Low	$4.67x10^3 \pm 0.34$	$1.33x10^5 \pm 0.11$	$0.23x10^6 \pm 0.02$
	ENC-VP8* Trivalent Mid	$1.46x10^4 \pm 0.05$	$8.95x10^5 \pm 0.05$	$3.43x10^6 \pm 0.05$
	ENC-VP8* Trivalent High	$1.82x10^4 \pm 0.07$	$1.55x10^6 \pm 0.25$	$4.29x10^6 \pm 0.05$

Cut off value was calculated as mean of negative serum at dilution 1:1000 + 3 x standard error

N.D had end point titer of less than 1000

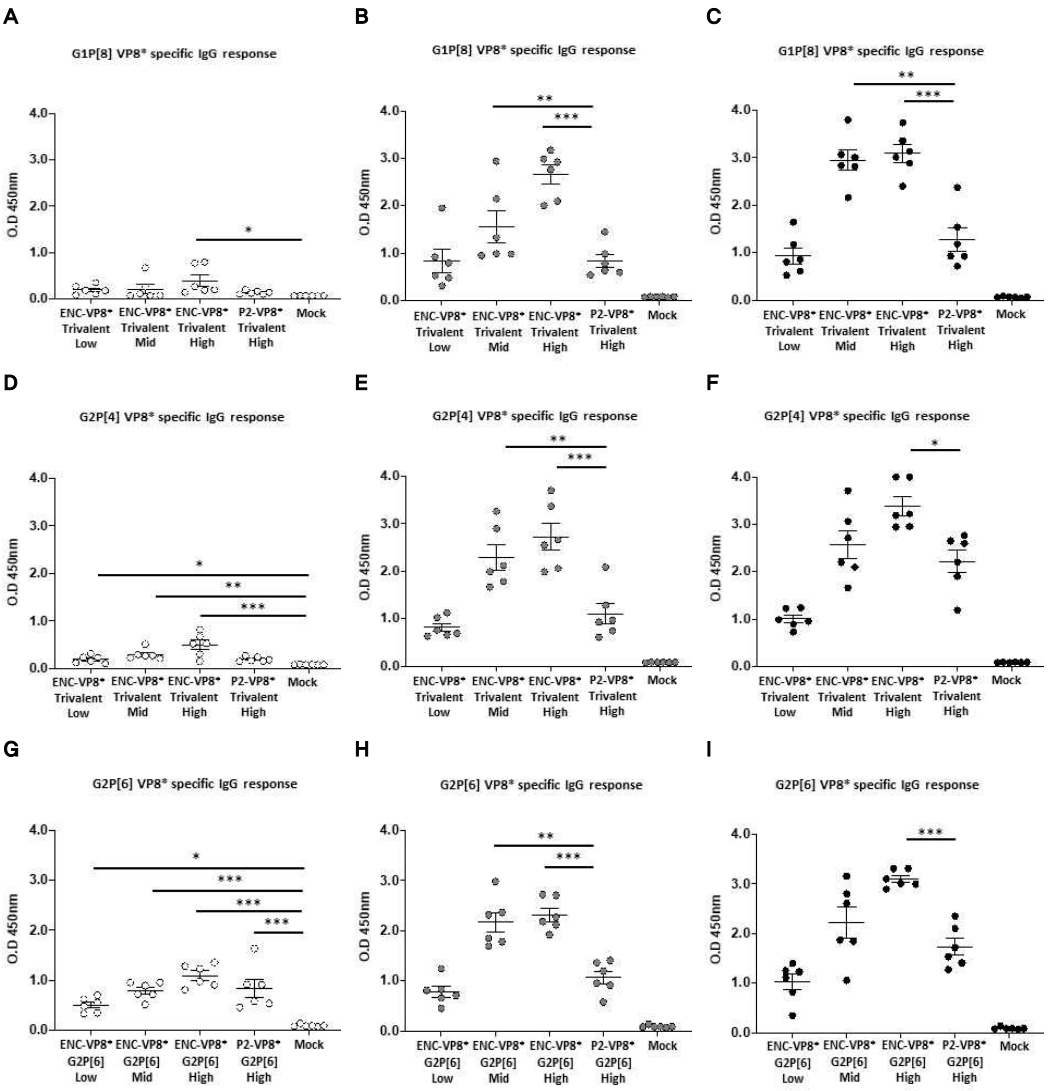

Fig 14. VP8* specific IgG response of the trivalent vaccine immunized individual mice sera

G1P[8]VP8* (A-C), G2P[4]VP8* (D-F) and G2P[6]VP8* (G-I) specific antibody responses in mice immune serum. BALB/C mice were immunized 3 times with trivalent P2-[4]VP8* or trivalent ENC-VP8*. Immune serum were diluted at 1:5000 ratio and added to recombinant protein VP8* coated

plate. VP8* antigen specific IgG were determined in prime (◯), Boost (●) and 2nd boost (●) immune serum. Statistically significant differences were further analyzed using T test. *P <0.05 **P < 0.01 and ***P < 0.005.

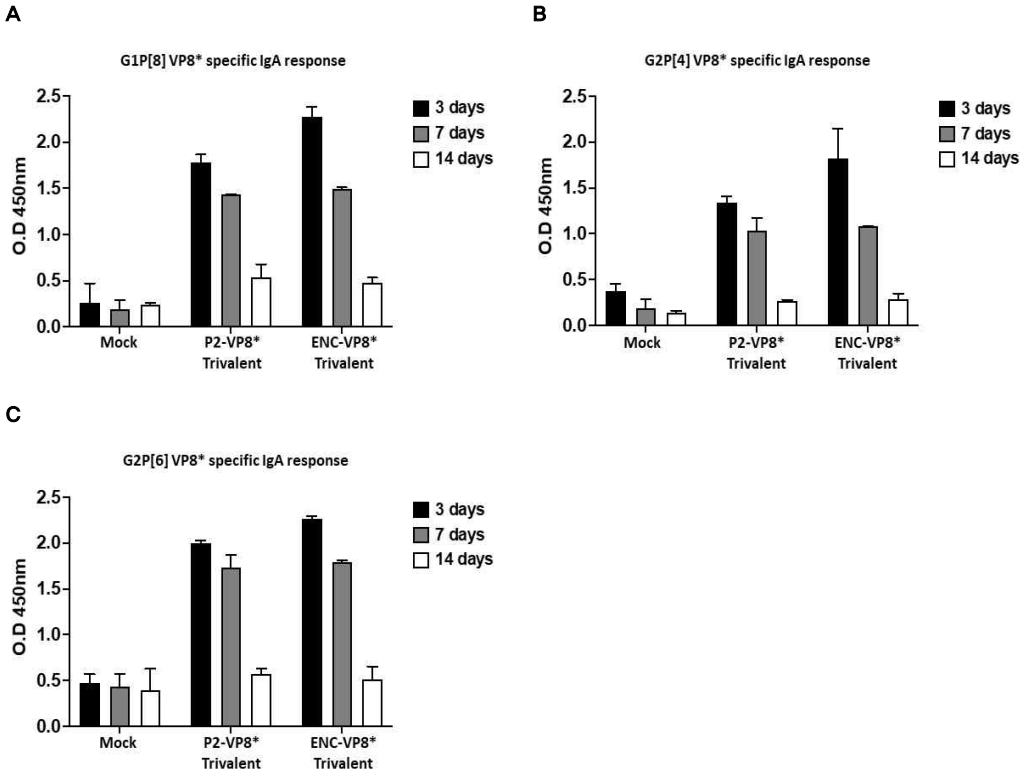

Fig. 15. VP8* specific IgA response of the trivalent vaccine

G1P[8]VP8* (A), G2P[4]VP8* (B) and G2P[6]VP8* (C) specific IgA responses in fecal extracts. Feces were collected from immunized mice in 3, 7 and 14 days after final immunization respectively. Levels of IgA in the feces were determined by ELISA.

VP8*-Led H type 1 binding inhibitory antibody response of the monovalent vaccine

To confirm that G1P[8], G2P[4], and G2P[6] of ENC-VP8* and P2-VP8* immune serum can inhibit binding between VP8* (rotavirus receptor binding domain) and cell surface receptors, the response to block the binding of VP8* and Led H type 1 was measured. In serum primed vaccination with G1P[8] VP8* monovalent vaccine, ENC-G1P[8]VP8* showed the highest blocking response to VP8* and Led H type 1 binding at 1:2000 dilution (Fig. 16A). The blocking dilution (BD_{50}) titer of ENC-G1P[8]VP8* was the highest and more than 8-folds higher than P2-G1P[8]VP8* (Table 8.). In the boost vaccination sera, mid and high doses of ENC-G1P[8]VP8* showed the highest blocking response at similar levels followed by low dose ENC-G1P[8]VP8* and P2-G1P[8]VP8* (Fig. 16B). After the final vaccination, mid and high doses of ENC-G1P[8]VP8* induced complete binding inhibition in immune sera diluted at a ratio of 1:32000 (Fig. 16C). P2-G1P[8]VP8* and low doses of ENC-G1P[8]VP8 had to be diluted at a ratio of 1:4000 and 1:8000, respectively, to induce complete binding inhibition (Fig. 16C). In BD_{50} titer, mid and high doses of ENC-G1P[8]VP8* were approximately 4 to 5-folds higher than that in P2-G1P[8]VP8*, while low doses of ENC-G1P[8]VP8 were approximately 1.5-folds higher than that in P2-G1P[8]VP8 (Table 8).

The G2P[4] VP8* vaccine was prime immunized, whereby mid and high doses of ENC-G2P[4]VP8* showed BD_{50} titer (Table 9). In immune sera diluted at a ratio of 1:2000, only a high dose of ENC-G2P[4]VP8* induced a weak blocking response (Fig. 17A). After the boost vaccination, the

blocking response in the ENC-G2P[4]VP8* immune serum (at 1:2000 dilution) increased significantly, showing 100% efficiency, however, P2-G2P[4]VP8* was weakly induced as well (Fig. 17B). Even after the final vaccination, the P2-G2P[4]VP8* immune serum (at 1:2000 dilution) did not show complete binding inhibition, however, a high dose of ENC-G2P[4]VP8* induced a complete binding inhibition up until a dilution at a rate of 1:8000 (Fig. 17C). BD_{50} titer showed that a high and low dose of ENC-G2P[4]VP8* were approximately 7-folds and 3-folds higher than P2-G2P[4]VP8*, respectively (Table 9)

In the G2P[6] VP8* vaccine immunization group, BD_{50} titer was induced in all groups except the low-dose ENC-G2P[6]VP8* in prime serum. Mid and high doses of ENC-G2P[6]VP8* showed a blocking response in serum diluted at a rate of 1:2000 (Table 10 and Fig. 18A). After the boost vaccination, only a high dose of ENC-G2P[6]VP8* immune sera (at 1:2000 dilution) induced complete binding inhibition, and a low dose of ENC-G2P[6]VP8* showed a lower blocking response than P2-G2P[6]VP8* (Fig. 18B). After the final vaccination, mid and high doses of ENC-G2P[6]VP8* induced a complete binding inhibition, however, low doses of ENC-G2P[6]VP8* and P2-G2P[6]VP8* did not show complete binding inhibition (Fig. 18C). The BD_{50} titer of high dose ENC-G2P[6]VP8* was approximately 4-folds higher than that of P2-G2P[6]VP8*, and a low dose of ENC-G2P[6]VP8* was similar to that of P2-G2P[6]VP8* (Table 10). These results indicate that monovalent G1P[8], G2P[4], and G2P[6] of ENC-VP8* vaccination induce an antibody response that selectively inhibits binding of VP8*-Led H type 1 as opposed to monovalent P2-VP8*.

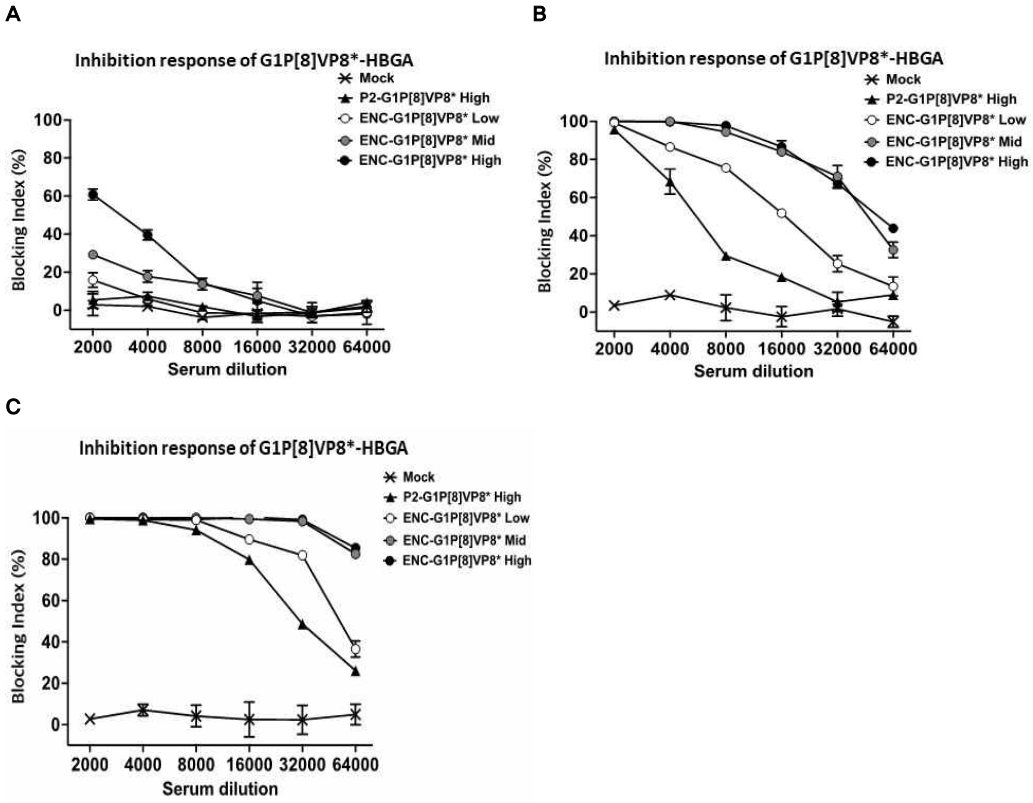

Fig 16. G1P[8]VP8*-Led H type 1 binding inhibitory response of G1P[8]VP8* monovalent vaccine

Inhibition responses of ENC-G1P[8]VP8* attachment to Led H type 1. ENC-G1P[8]VP8* at a concentration of 2 μg/mL were incubated with diluted immune serum. ENC-VP8*/serum mixtures were added to Led H type 1 coated plate. Attached ENC-G1P[8]VP8* were detected by specific rabbit antibody. Inhibition responses of HBGA binding in prime (A), Boost (B) and 2nd boost (C) immune sera.

Table 8. BD_{50} titer of G1P[8]VP8* monovalent vaccine immunized sera

Group	BD_{50} titer		
	Prime	Boost	2nd Boost
Mock	N.D	N.D	N.D
P2-VP8*(G1P[8]) High	$0.38x10^3 \pm 0.07$	$0.62x10^4 \pm 0.03$	$3.51x10^4 \pm 0.03$
ENC -VP8*(G1P[8]) Low	$0.72x10^3 \pm 0.07$	$1.59x10^4 \pm 0.18$	$5.72x10^4 \pm 0.02$
ENC -VP8*(G1P[8]) Mid	$2.57x10^3 \pm 0.16$	$4.70x10^4 \pm 0.41$	$1.38x10^5 \pm 0.22$
ENC -VP8*(G1P[8]) High	$2.89x10^3 \pm 0.04$	$5.51x10^4 \pm 0.26$	$1.72x10^5 \pm 0.36$

N.D had BD_{50} titer of less than 250

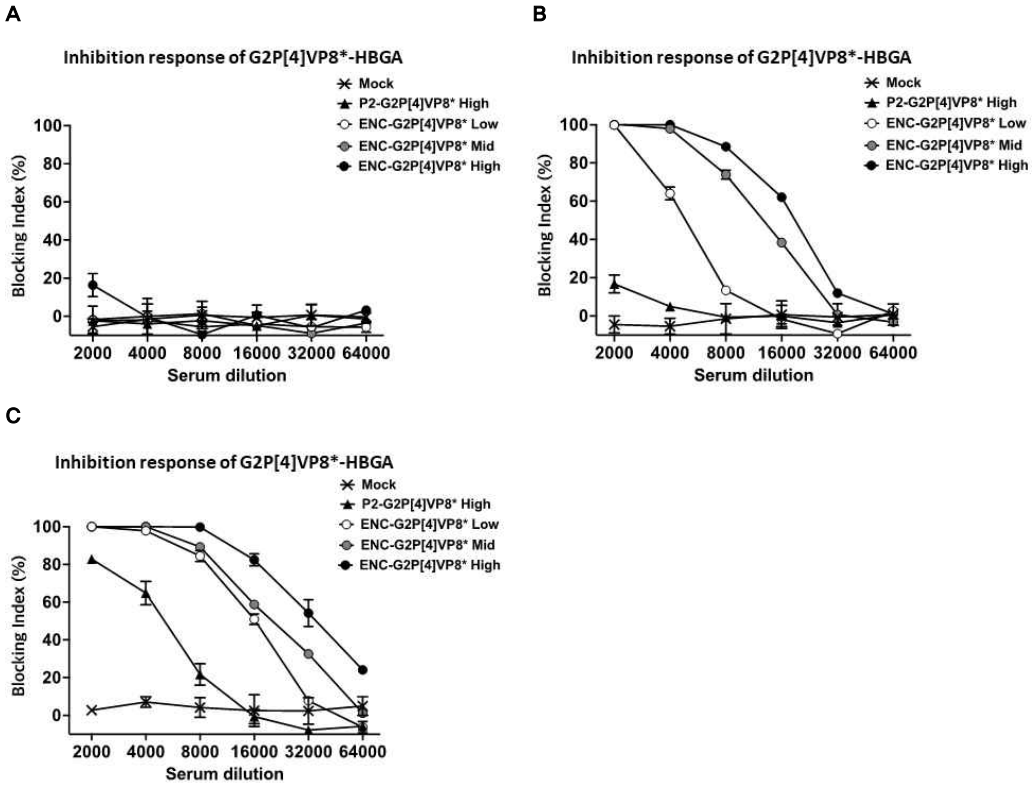

Fig. 17. G2P[4]VP8*-Led H type 1 binding inhibitory response of G2P[4]VP8* monovalent vaccine

Inhibition responses of ENC-G2P[4]VP8* attachment to Led H type 1. ENC-G2P[4]VP8* at a concentration of 2 μg/mL were incubated with diluted immune serum. ENC-VP8*/serum mixtures were added to Led H type 1 coated plate. Attached ENC-G2P[4]VP8* were detected by specific rabbit antibody. Inhibition responses of HBGA binding in prime (A), Boost (B) and 2nd boost (C) immune sera.

Table 9. BD_{50} titer of G2P[4]VP8* monovalent vaccine immunized sera

Group	BD_{50} titer		
	Prime	Boost	2nd Boost
Mock	N.D	N.D	N.D
P2-VP8*(G2P[4]) High	N.D	$0.91x10^3 \pm 0.05$	$0.51x10^4 \pm 0.11$
ENC-VP8*(G2P[4]) Low	N.D	$5.37x10^3 \pm 0.03$	$1.53x10^4 \pm 0.06$
ENC-VP8*(G2P[4]) Mid	$2.97x10^2 \pm 0.58$	$1.27x10^4 \pm 0.03$	$2.05x10^4 \pm 0.07$
ENC-VP8*(G2P[4]) High	$5.31x10^2 \pm 0.76$	$1.73x10^4 \pm 0.01$	$3.49x10^4 \pm 0.35$

N.D had BD_{50} titer of less than 250

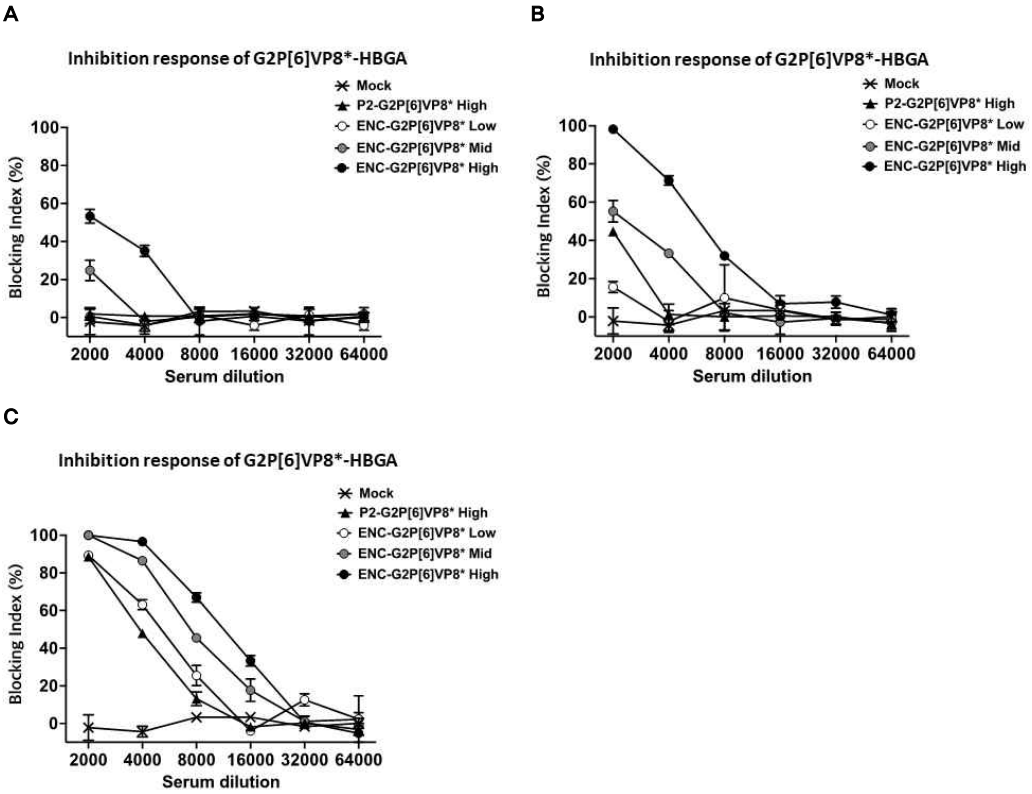

Fig. 18. G2P[6]VP8*-Led H type 1 binding inhibitory response of G2P[6]VP8* monovalent vaccine

Inhibition responses of ENC-G2P[6]VP8* attachment to Led H type 1. ENC-G2P[6]VP8* at a concentration of 2 μg/mL were incubated with diluted immune serum. ENC-VP8*/serum mixtures were added to Led H type 1 coated plate. Attached ENC-G2P[6]VP8* were detected by specific rabbit antibody. Inhibition responses of HBGA binding in prime (A), Boost (B) and 2nd boost (C) immune sera.

Table 10. BD_{50} titer of G2P[6]VP8* monovalent vaccine immunized sera

Group	BD_{50} titer		
	Prime	Boost	2nd Boost
Mock	N.D	N.D	N.D
P2-VP8*(G2P[6]) High	$0.41x10^3 \pm 0.03$	$1.85x10^3 \pm 0.07$	$4.81x10^3 \pm 0.12$
ENC-VP8*(G2P[6]) Low	N.D	$0.99x10^3 \pm 0.01$	$5.12x10^3 \pm 0.25$
ENC-VP8*(G2P[6]) Mid	$0.97x10^3 \pm 0.05$	$2.53x10^3 \pm 0.17$	$8.08x10^3 \pm 0.51$
ENC-VP8*(G2P[6]) High	$2.23x10^3 \pm 0.33$	$5.77x10^3 \pm 0.12$	$1.72x10^4 \pm 0.36$

N.D had BD_{50} titer of less than 250

VP8*-Led H type 1 binding inhibitory antibody response of the trivalent vaccine

The ability of trivalent vaccine immune serum to inhibit the binding of G1P[8], G2P[4], and G2P[6] VP8* serotypes to Led H type 1 was confirmed using HBGA blocking assay. The blocking response of VP8* G1P[8] serotype was evident only in high doses of trivalent ENC-VP8* in prime serum, however, there was no response after dilution at a ratio of 1:2000 (Table 11 Fig. 19A). In boost immunized sera, the blocking response was induced in all immunized mice, whereby mid and high doses of trivalent ENC-VP8* showed higher binding inhibition ability than trivalent P2-VP8* (Table 11 and Fig. 19B). After the final vaccination, mid and high doses of trivalent ENC-VP8* showed higher binding inhibition ability than trivalent P2-VP8*, mid doses of ENC-VP8* and high doses of trivalent ENC-VP8* showed approximately 1.5-folds and 3-folds higher BD_{50} values, respectively (Table 11 and Fig. 19C). Additionally, a low dose of trivalent ENC-VP8* induced a blocking response similar to that of trivalent P2-VP8* (Table 11 and Fig. 19C). The reaction that inhibited binding of G2P[4] VP8* was weakly induced only in high doses of trivalent ENC-VP8* in prime sera (Fig. 19D) In boost vaccinations, the blocking response was shown in all immunized mice, whereby the trivalent ENC-VP8* immunized group induced a higher blocking response than that of trivalent P2-VP8* (Fig. 19E). After the final vaccination, a low, mid, and high dose of ENC-VP8* induced a blocking response approximately 2, 3, and 6-folds higher than that of trivalent P2-VP8*, respectively (Table 11). Responses from inhibiting binding to G1P[6] VP8* appeared in all prime immunized mice,

whereby a high dose trivalent ENC-VP8* induced the highest blocking response (Table 11 and Fig. 19G). After the boost vaccination, blocking responses increased where a mid and high dose of trivalent ENC-VP8* showed higher binding inhibition ability than that of trivalent P2-VP8* (Fig. 19H). BD_{50} titers showed A mid and high dose of trivalent ENC-VP8* showed approximately 1.5 and 2-fold higher BD_{50} titer than that of trivalent P2-VP8*, respectively (Table 11). After the final vaccination, the BD50 titer increased by more than 2-folds (Table 11). A high dose of trivalent ENC-VP8* induced a higher blocking response than that of trivalent P2-VP8*. Similarly, a low and mid dose of trivalent ENC-VP8* induced to a similar level (Fig. 19I). These results show that the trivalent VP8* vaccine-induced antibodies that inhibit binding to VP8*-Led H type 1, whereby the trivalent ENC-VP8* vaccine induced a higher blocking response than that of trivalent P2-VP8*.

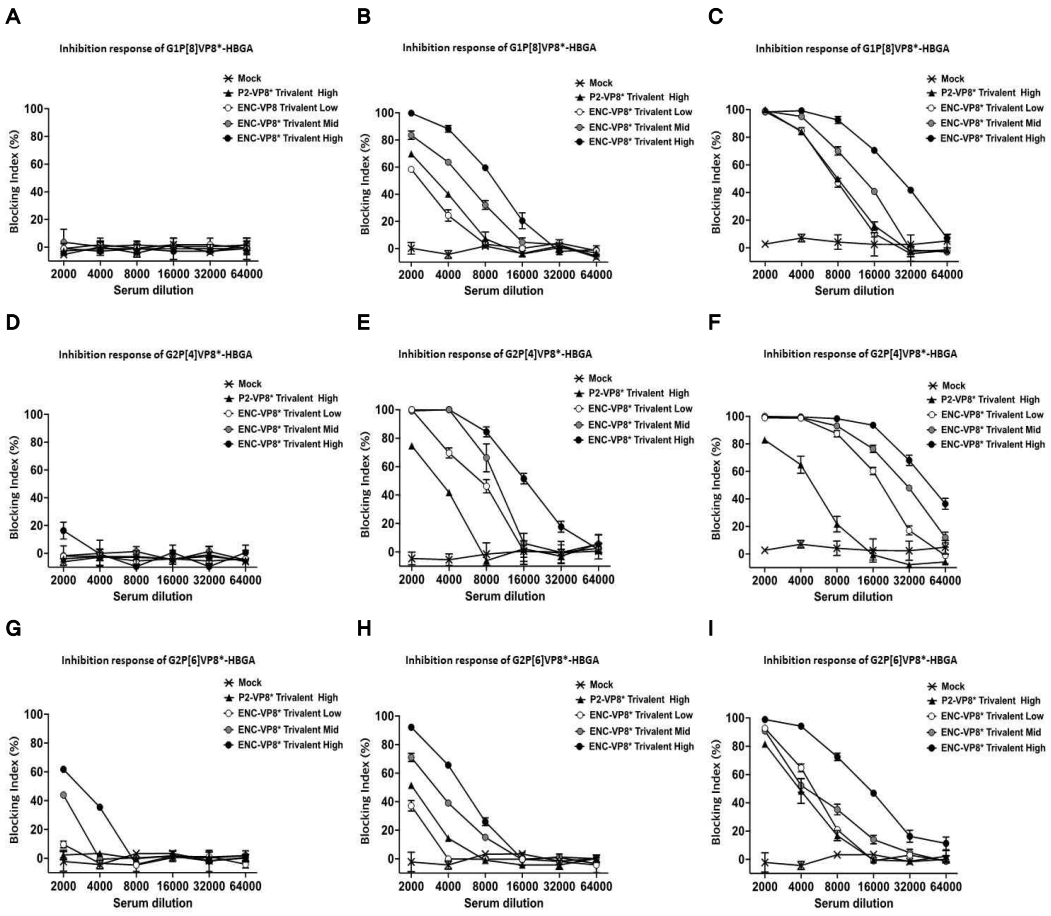

Fig. 19. VP8*-Led H type 1 binding inhibitory response of the trivalent vaccine

Inhibition responses of ENC-G1P[8]VP8* (A-C), ENC-G2P[4]VP8* (D-F) and ENC-VP8* (G-I) attachment to Led H type 1. Three serotype of ENC-VP8* at a concentration of 2 μg/mL were incubated with diluted immune serum. ENC-VP8*/serum mixtures were added to Led H type 1 coated plate. Attached ENC-VP8* were detected by specific rabbit antibody. Inhibition responses of HBGA binding in prime (A, D, G), Boost (B, E, H) and 2nd boost (C, F, I) immune sera.

Table 11. BD_{50} titer of the trivalent vaccine immunized sera

VLP	Group	BD50 titer		
		Prime	Boost	2nd Boost
G1P[8] VLP	Mock	N.D	N.D	N.D
	P2-VP8* Trivalent High	N.D	$3.13x10^3 \pm 0.11$	$8.02x10^3 \pm 0.25$
	ENC-VP8* Trivalent Low	N.D	$2.45x10^3 \pm 0.14$	$7.63x10^3 \pm 0.23$
	ENC-VP8* Trivalent Mid	N.D	$5.21x10^3 \pm 0.51$	$1.22x10^4 \pm 0.07$
	ENC-VP8* Trivalent High	$3.17x10^2 \pm 0.27$	$9.09x10^3 \pm 0.43$	$2.55x10^4 \pm 0.04$
G2P[4] VLP	Mock	N.D	N.D	N.D
	P2-VP8* Trivalent High	$2.61x10^2 \pm 0.15$	$3.18x10^3 \pm 0.03$	$7.72x10^3 \pm 0.02$
	ENC-VP8* Trivalent Low	N.D	$6.36x10^3 \pm 0.72$	$1.76x10^4 \pm 0.06$
	ENC-VP8* Trivalent Mid	$3.82x10^2 \pm 0.04$	$8.95x10^3 \pm 0.09$	$2.89x10^4 \pm 0.19$
	ENC-VP8* Trivalent High	$9.81x10^2 \pm 0.18$	$1.64x10^4 \pm 0.15$	$4.69x10^4 \pm 0.19$
G2P[6] VLP	Mock	N.D	N.D	N.D
	P2-VP8* Trivalent High	$0.74x10^3 \pm 0.05$	$1.93x10^3 \pm 0.03$	$3.91x10^3 \pm 0.04$
	ENC-VP8* Trivalent Low	$0.81x10^3 \pm 0.05$	$1.51x10^3 \pm 0.05$	$4.82x10^3 \pm 0.01$
	ENC-VP8* Trivalent Mid	$1.62x10^3 \pm 0.11$	$2.89x10^3 \pm 0.06$	$5.12x10^3 \pm 0.06$
	ENC-VP8* Trivalent High	$2.68x10^3 \pm 0.04$	$5.07x10^3 \pm 0.15$	$1.42x10^4 \pm 0.04$

N.D had BD_{50} titer of less than 250

Rotavirus neutralization antibody response of the monovalent vaccine

We evaluated the potency of G1P[8], G2P[4], and G2P[6] VP8* monovalent vaccine in inducing neutralizing antibody responses against the human rotavirus. In the boost immunized sera, mid and high doses of ENC-G1P[8]VP8* induced a strong neutralizing antibody response to the rotavirus WA strain (G1P[8]). Similarly, a low dose of ENC-G1P[8]VP8* and P2-G1P[8]VP8* induced similar levels of neutralizing response (Table 12 and Fig. 20A). After the final vaccination, the neutralizing antibody response increased and ENC-G1P[8]VP8* induced a higher neutralizing antibody response than that of P2-G1P[8]VP8* (Fig. 20B). $PRNT_{50}$ titer showed that a high, mid, and low dose of ENC-G1P[8]VP8* was induced a neutralizing antibody response approximately 4, 3, and 2-folds higher than that of P2-G1P[8]VP8*, respectively (Table 12).

The G2P[4] VP8* vaccine was able to neutralize the rotavirus DS-1 strain after the boost vaccination. A high dose of ENC-G2P[4]VP8* induced the highest neutralizing antibody (Fig. 21A), where the $PRNT_{50}$ titer was approximately 3-folds higher than that of P2-G2P[4]VP8* (Table 13). After the final vaccination, the $PRNT_{50}$ titer increased approximately 2-folds, whereby a high dose of ENC-G2P[4]VP8* still showed a higher neutralizing antibody response than that of P2-G2P[4]VP8* (Table 13 and Fig. 21B). A mid dose of ENC-G2P[4]VP8* showed a slightly lower neutralizing antibody response than that of P2-G2P[4]VP8*. Finally, a low dose of ENC-G2P[4]VP8* showed a low neutralizing antibody response (Table 13 and Fig. 21B).

After the boost immunization of the G2P[6] VP8* vaccine, a high dose of ENC-G2P[6]VP8* showed the highest neutralizing antibody response and approximately 2-fold higher $PRNT_{50}$ titer than that of P2-G2P[6]VP8* (Table 14 and Fig. 22A). After the final vaccination, the neutralizing antibody responses were approximately doubled. A high dose of ENC-G2P[6]VP8* still showed a higher neutralizing antibody response than that of P2-G2P[6]VP8* (Table 14 and Fig. 22B). However, low and mid doses of ENC-G2P[6]VP8* induced a weak neutralizing antibody response than that of P2-G2P[6]VP8* (Table 14 and Fig. 22B). These results show that G1P[8], G2P[4], and G2P[6] monovalent vaccine immunization induce neutralizing antibodies against the rotavirus, whereby ENC-VP8* exhibits a higher neutralizing antibody response than that of P2-VP8*.

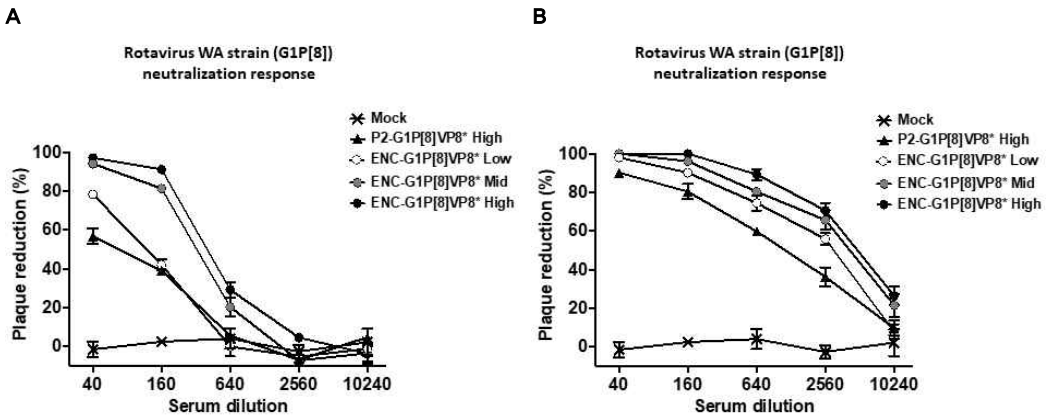

Fig. 20. G1P[8] virus neutralizing antibody response of G1P[8]VP8* monovalent vaccine

Plaque reduction neutralization assay. rotavirus Wa strain (G1P[8]) were incubated with G1P[8] vaccine immune serum and infected with MA 104 cell. Plaques were counted after 5 days. Inhibitory response of boost (A) and 2nd boost (B) immune serum to rotavirus plaque forming.

Table 12. $PRNT_{50}$ titer of G1P[8]VP8* monovalent vaccine immunized sera

Group	$PRNT_{50}$ titer	
	Boost	2^{nd} Boost
Mock	N.D	N.D
P2-VP8*(G1P[8]) High	$1.04x10^2 \pm 0.01$	$1.03x10^3 \pm 0.03$
ENC-VP8*(G1P[8]) Low	$1.02x10^2 \pm 0.03$	$2.21x10^3 \pm 0.07$
ENC-VP8*(G1P[8]) Mid	$3.72x10^2 \pm 0.05$	$3.83x10^3 \pm 0.09$
ENC-VP8*(G1P[8]) High	$5.47x10^2 \pm 0.13$	$4.91x10^3 \pm 0.11$

N.D had $PRNT_{50}$ titer of less than 10

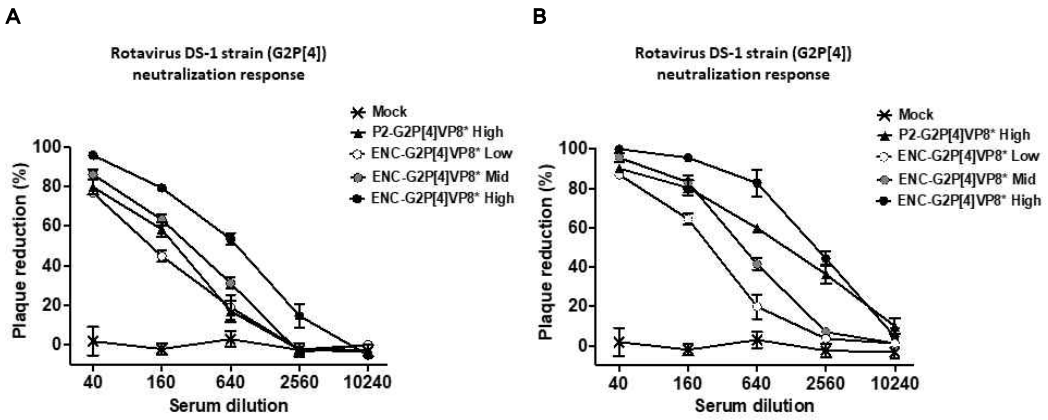

Fig. 21. G2P[4] virus neutralizing antibody response of G2P[4]VP8* monovalent vaccine

Plaque reduction neutralization assay. rotavirus DS-1 strain (G2P[4]) were incubated with G2P[4] vaccine immune serum and infected with MA 104 cell. Plaques were counted after 5 days. Inhibitory response of boost (A) and 2nd boost (B) immune serum to rotavirus plaque forming.

Table 13. $PRNT_{50}$ titer of G2P[4]VP8* monovalent vaccine immunized sera

Group	$PRNT_{50}$ titer	
	Boost	2^{nd} Boost
Mock	N.D	N.D
P2-VP8*(G2P[4]) High	$1.94x10^2 \pm 0.06$	$5.36x10^2 \pm 0.03$
ENC-VP8*(G2P[4]) Low	$1.42x10^2 \pm 0.03$	$2.41x10^2 \pm 0.08$
ENC-VP8*(G2P[4]) Mid	$2.72x10^2 \pm 0.05$	$5.14x10^3 \pm 0.08$
ENC-VP8*(G2P[4]) High	$6.28x10^2 \pm 0.12$	$2.05x10^3 \pm 0.05$

N.D had $PRNT_{50}$ titer of less than 10

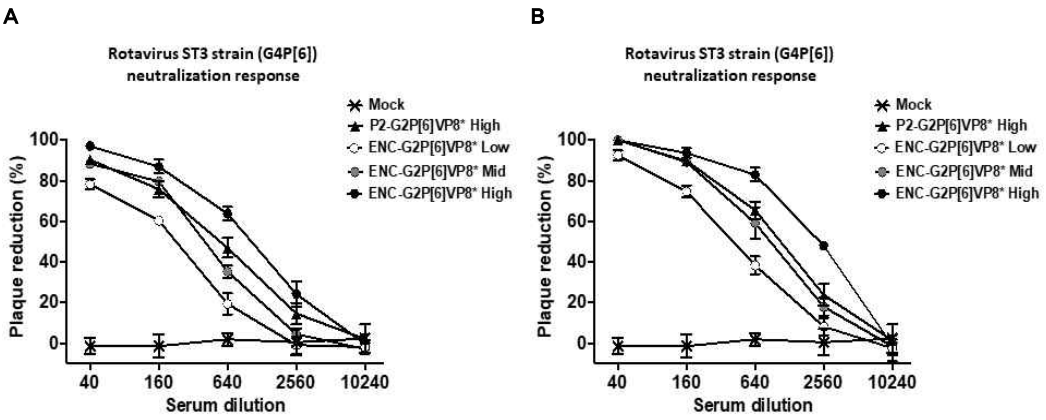

Fig. 22. G4P[6] virus neutralizing antibody response of G2P[6]VP8* monovalent vaccine

Plaque reduction neutralization assay. rotavirus ST3 strain (G4P[6]) were incubated with G2P[6] vaccine immune serum and infected with MA 104 cell. Plaques were counted after 5 days. Inhibitory response of boost (A) and 2nd boost (B) immune serum to rotavirus plaque forming.

Table 14. $PRNT_{50}$ titer of G2P[6]VP8* monovalent vaccine immunized sera

Group	$PRNT_{50}$ titer	
	Boost	2^{nd} Boost
Mock	N.D	N.D
P2-VP8*(G2P[6]) High	$5.31x10^2 \pm 0.04$	$9.69x10^2 \pm 0.06$
ENC-VP8*(G2P[6]) Low	$1.96x10^2 \pm 0.02$	$4.28x10^2 \pm 0.01$
ENC-VP8*(G2P[6]) Mid	$4.45x10^2 \pm 0.03$	$7.83x10^2 \pm 0.04$
ENC-VP8*(G2P[6]) High	$9.42x10^2 \pm 0.17$	$2.05x10^3 \pm 0.05$

N.D had $PRNT_{50}$ titer of less than 10

Rotavirus neutralization antibody response of the trivalent vaccine

The neutralizing antibody responses to the rotavirus WA (G1P[8]), DS-1 (G2P[4]), and ST3 (G4P[6]) strains induced by the trivalent VP8* vaccine were measured with the PRNT assay. After the boost vaccination, it was confirmed that a neutralizing antibody response was induced against the rotavirus WA strain infection, whereby mid and high doses of trivalent ENC-VP8* induced a higher neutralizing antibody response than that of trivalent P2-VP8* (Fig. 23A). A high and mid dose of trivalent ENC-VP8* showed a higher $PRNT_{50}$ titer by approximately 7 and 3-folds than that of trivalent P2-VP8*, respectively (Table 15). After the final vaccination, neutralizing antibody responses to the rotavirus Wa strain increased, where a high dose of trivalent ENC-VP8* induced a neutralizing antibody response approximately 3-folds higher than that of trivalent P2-VP8* (Table 15 and Fig. 23B). Similarly, a mid-dose of trivalent ENC-VP8* showed similar levels of neutralizing antibody response to trivalent P2-VP8*, whereas a low dose of trivalent ENC-VP8* induced a low neutralizing antibody response (Fig. 23B). The neutralizing antibody response to the rotavirus DS-1 strain was induced after the boost immunization with the trivalent VP8* vaccine (Fig. 23C and D). A high dose of trivalent ENC-VP8* induced a neutralizing antibody response approximately 4-folds higher than that of trivalent P2-VP8* (Table 15). In the final immunized mice sera, the neutralizing antibody response of the trivalent P2-VP8* increased by approximately 10-folds, however, still showing a weak neutralizing antibody response when compared to the high

dose of trivalent ENC-VP8* (Table 15 and Fig. 23D). On the other hand, the trivalent P2-VP8* induced a higher neutralizing antibody response than that of the low and mid doses of trivalent ENC-VP8* (Table 15). Additionally, the neutralizing antibody response was also induced against the rotavirus ST3 strain after the boost vaccination, whereby a high dose of trivalent ENC-VP8* showed the highest neutralizing antibody response (Table 15, Fig. 23E, and F). In the final immunized mice sera, the neutralizing antibody response against the rotavirus ST3 strain increased, completely suppressing the viral infection in diluted mice sera at a rate of 1:40 (Fig. 23F). A high dose of trivalent ENC-VP8* still showed the highest neutralizing antibody response, and the mid dose of trivalent ENC-VP8* and P2-VP8* induced similar levels of neutralizing antibody response (Table 15 and Fig 23F). As a result, it was confirmed that the trivalent VP8* vaccine induces neutralizing antibodies that inhibit the rotavirus infection from the G1P[8], G2P[4], and G4P[6] serotypes. Notably, the trivalent ENC-VP8* induced a higher neutralizing antibody response than that of trivalent P2-VP8*.

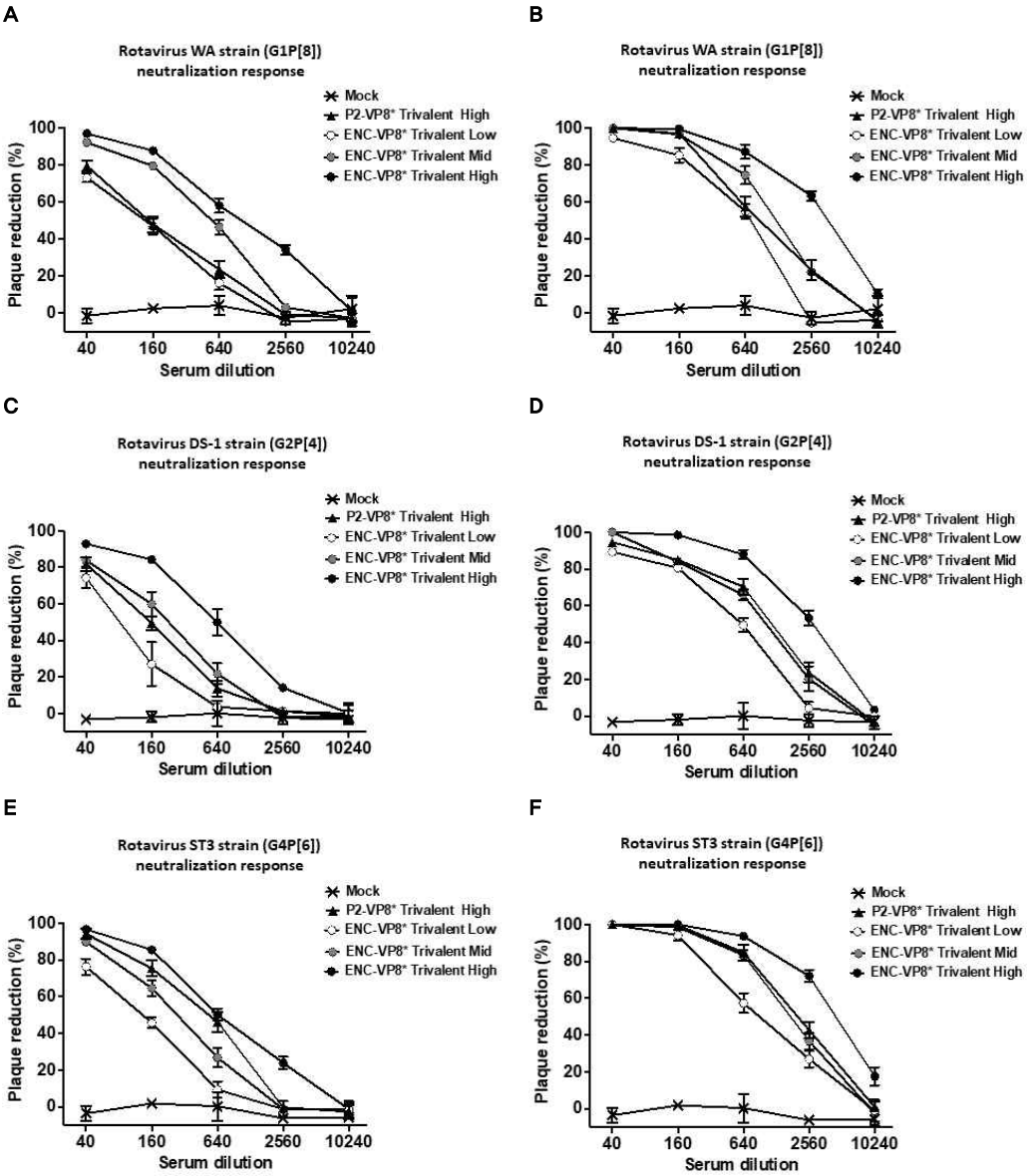

Fig 23. Three serotypes of rotavirus neutralizing antibody response of the trivalent vaccine

Plaque reduction neutralization assay. Three serotype of rotavirus were incubated with trivalent vaccine immune serum and infected with MA 104

cell. Plaques were counted after 5 days. Inhibitory response of boost (A,C,E) and 2nd boost (B,D,F) immune serum to rotavirus WA (A-B), DS-1 (C-D) and ST3 (E-F) strain plaque forming.

Table 15. $PRNT_{50}$ titer of the trivalent vaccine immunized sera

Virus	Group	$PRNT_{50}$ titer	
		Boost	2nd Boost
Wa G1P[8]	Mock	N.D	N.D
	P2-VP8* Trivalent High	$1.65x10^2 \pm 0.14$	$1.08x10^3 \pm 0.21$
	ENC-VP8* Trivalent Low	$1.29x10^2 \pm 0.11$	$5.47x10^2 \pm 0.06$
	ENC-VP8* Trivalent Mid	$4.98x10^2 \pm 0.15$	$1.24x10^3 \pm 0.26$
	ENC-VP8* Trivalent High	$1.01x10^3 \pm 0.23$	$2.93x10^3 \pm 0.46$
DS-1 G2P[4]	Mock	N.D	N.D
	P2-VP8* Trivalent High	$1.50x10^2 \pm 0.13$	$1.16x10^3 \pm 0.15$
	ENC-VP8* Trivalent Low	$0.91x10^2 \pm 0.03$	$5.35x10^2 \pm 0.15$
	ENC-VP8* Trivalent Mid	$2.08x10^2 \pm 0.17$	$9.86x10^2 \pm 0.38$
	ENC-VP8* Trivalent High	$6.34x10^2 \pm 0.19$	$2.41x10^3 \pm 0.25$
ST3 G4P[6]	Mock	N.D	N.D
	P2-VP8* Trivalent High	$4.49x10^2 \pm 0.09$	$2.02x10^3 \pm 0.29$
	ENC-VP8* Trivalent Low	$1.22x10^2 \pm 0.12$	$9.65x10^2 \pm 0.26$
	ENC-VP8* Trivalent Mid	$2.81x10^2 \pm 0.17$	$1.82x10^3 \pm 0.11$
	ENC-VP8* Trivalent High	$7.38x10^2 \pm 0.24$	$3.89x10^3 \pm 0.19$

N.D had $PRNT_{50}$ titer of less than 10

Virus-specific T-cell response of the monovalent vaccine

T-cell responses induced by the monovalent ENC-VP8* and P2-VP8* vaccine candidates after virus stimulation were confirmed using the ELISpot assay. The G1P[8] VP8* vaccine induced both IL-4 and IFN-γ responses. The response induced by ENC-G1P[8]VP8* was 1.5-folds higher than that of P2-G1P[8]VP8* (Fig. 24). The IFN-γ response induced by inoculating the G2P[4] VP8* vaccine showed a statistically significant level of ENC-G2P[4]VP8* compared to P2-G2P[4]VP8*. However, the IL-4 response was induced to a similar level (Fig. 25). After immunization by the G2P[6] VP8* vaccine, the IFN-γ response induced by ENC-G2P[6]VP8* was 2-fold higher than that of P2-G2P[6]VP8*. Additionally, the IL-4 response induced by ENC-G2P[6]VP8* was higher than that of P2-G2P[6]VP8* with statistical significance (Fig. 26). As a result, it was confirmed that the monovalent VP8* vaccine induced IFN-γ and IL-4 secretions as part of the T-cell response. Moreover, the ENC-VP8* vaccine induced both IL-4 and IFN-γ responses to a higher level when compared to the P2-VP8* vaccine.

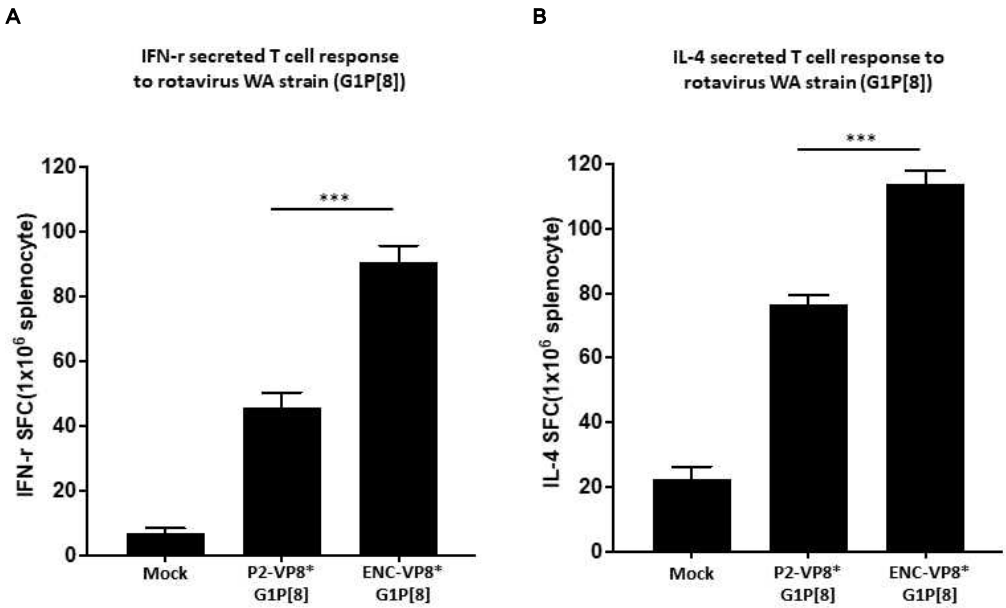

Fig. 24. T-cell response of G1P[8]VP8* monovalent vaccine

Cellular immune responses by G1P[8] VP8* vaccine immunization. Splenocytes were isolated from ENC-G1P[8]VP8* or P2-G1P[8]VP8* Immunized mice and IFN-γ (A) or IL-4 (B) secreting cells were quantified using an ELISPOT assay. Statistically significant differences were analyzed using T test. ***$P < 0.005$.

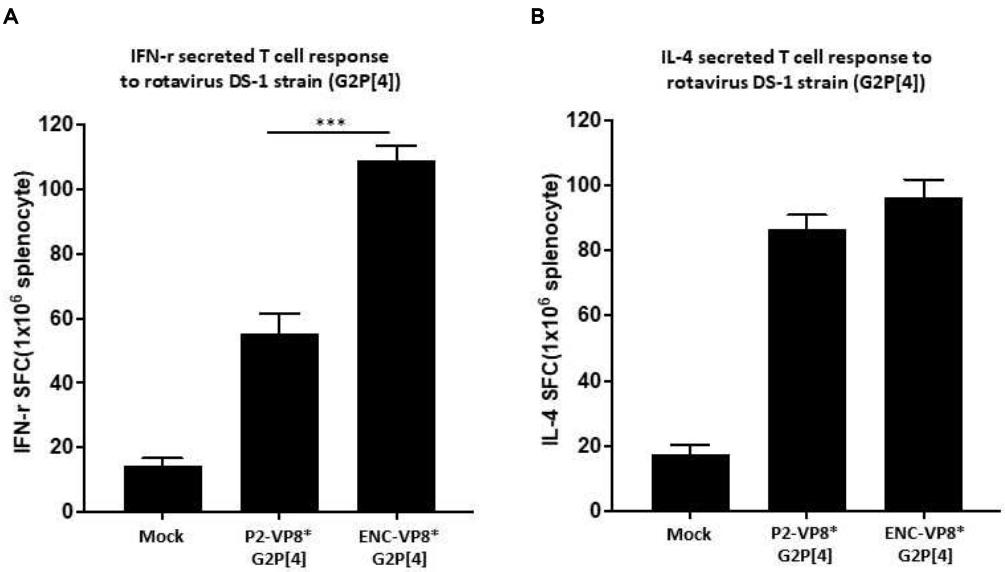

Fig. 25. T-cell response of G2P[4]VP8* monovalent vaccine

Cellular immune responses by G2P[4] VP8* vaccine immunization. Splenocytes were isolated from ENC-G2P[4]VP8* or P2-G2P[4]VP8* Immunized mice and IFN-γ (A) or IL-4 (B) secreting cells were quantified using an ELISPOT assay. Statistically significant differences were analyzed using T test. ***$P < 0.005$.

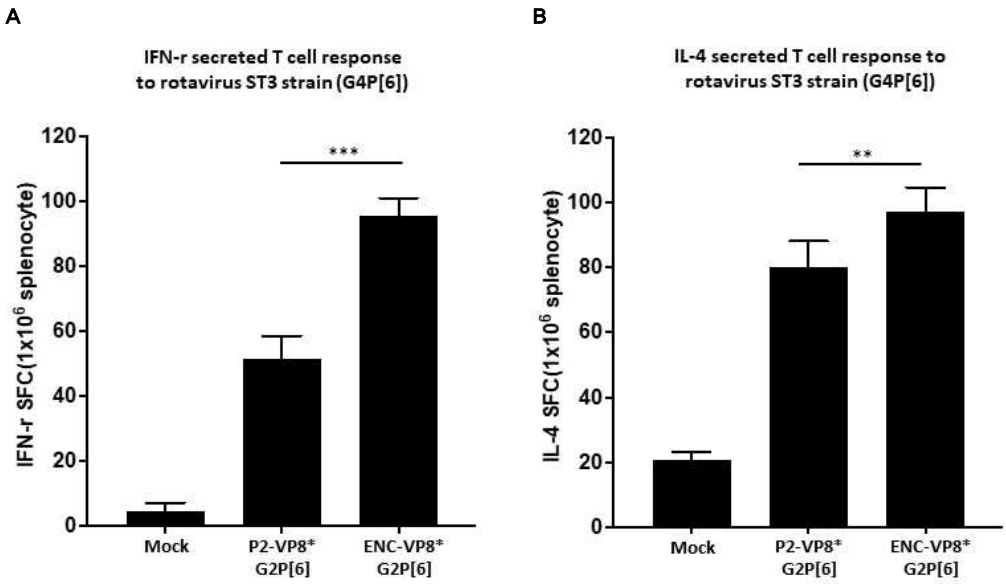

Fig. 26. T-cell response of G2P[6]VP8* monovalent vaccine

Cellular immune responses by G2P[6] VP8* vaccine immunization. Splenocytes were isolated from ENC-G2P[6]VP8* or P2-G2P[6]VP8* Immunized mice and IFN-γ (A) or IL-4 (B) secreting cells were quantified using an ELISPOT assay. Statistically significant differences were analyzed using T test. $^{**}P < 0.01$ and $^{***}P < 0.005$.

Virus-specific T-cell response of the trivalent vaccine

T-cell responses induced by the Trivalent VP8* vaccine after virus stimulation was confirmed using the ELISPOT assay. The IFN-γ response against the G1P[8] virus was higher when induced by the trivalent ENC-VP8* as compared to the trivalent P2-VP8*, however, both induced similar IL-4 responses (Fig. 27A and B). After inoculation of the G2P[4] virus, the trivalent ENC-VP8* induced a higher IFN-γ response than that of the trivalent P2-VP8* with statistical significance. However, the IL-4 response showed no statistically significant difference (Fig. 27C and D). For the G4P[6] virus, the trivalent ENC-VP8* induced a statistically significant higher IFN-γ and IL-4 response by approximately 1.5 and 2-fold than that of trivalent P2-VP8*, respectively (Fig. 27 E and F). As a result, it was confirmed that the trivalent VP8* vaccine can induce IFN-γ and IL-4 responses, whereby ENC-VP8* induced IFN-γ and IL-4 responses against rotavirus G1P[8], G2P[4], and G4P[6] serotypes.

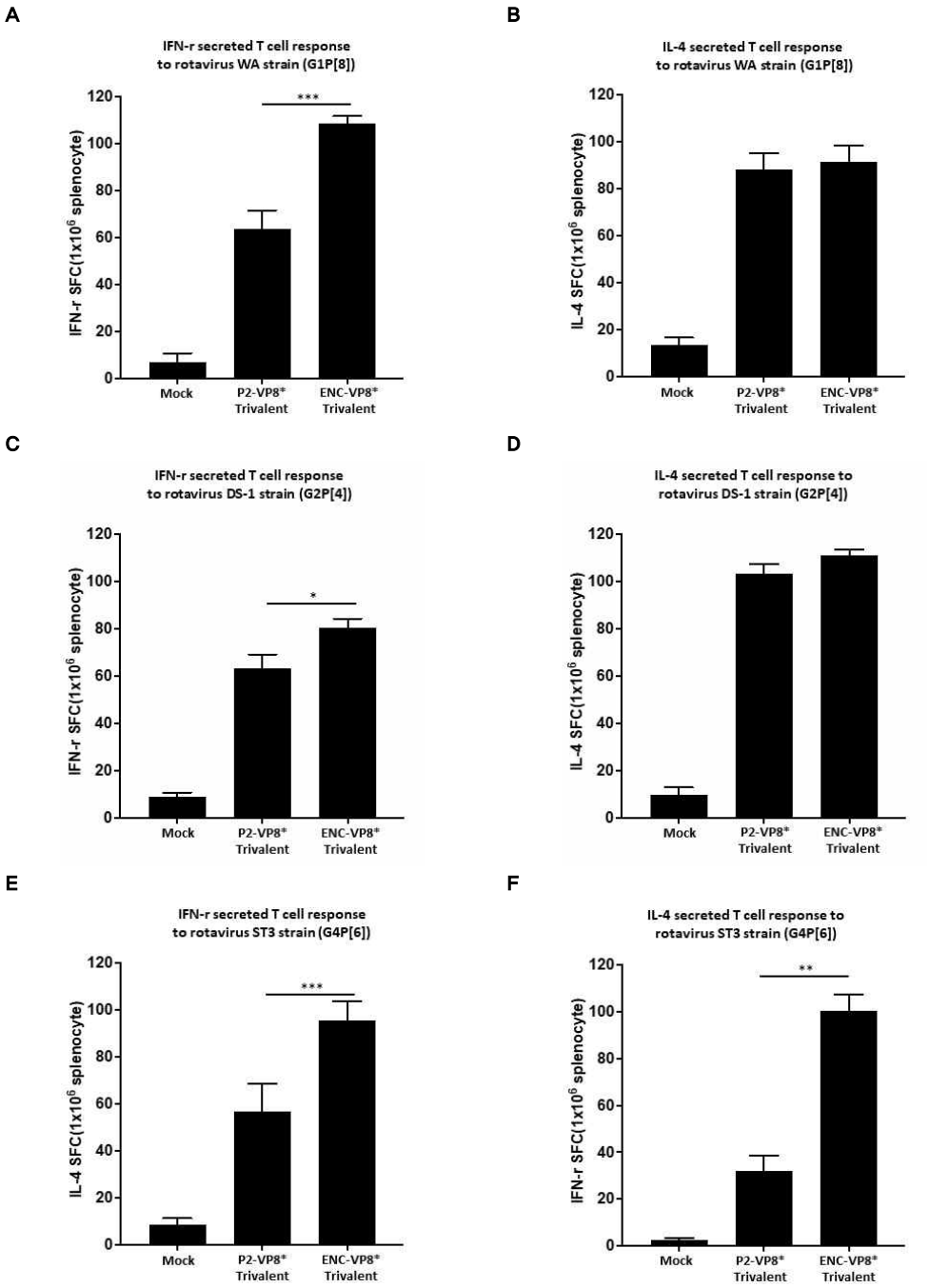

Fig. 24. T-cell response of the trivalent vaccine

Cellular immune responses by trivalent VP8* vaccine immunization.

Splenocytes were isolated from trivalent ENC-VP8* or trivalent P2-VP8* Immunized mice and IFN-γ (A, C, E) or IL-4 (B, D, F) secreting cells were quantified using an ELISPOT assay. Statistically significant differences were analyzed using T test. *$P < 0.05$ and **$P < 0.01$.

Discussion

In rotavirus, the VP8* protein is the standard for dividing the P serotypes and attaches to host cells to initiate infection [68,69]. VP8* is a vaccine candidate to effectively prevent infection by the rotavirus [70]. However, because subunits alone do not induce a sufficient immune response, the universal tetanus toxin $CD4^+$ T-cell epitope (P2) was expressed in the N terminal of VP8* or VP4 protein before it was divided into VP5* and VP8*, to enhance immunogenicity [37,71]. Recently, studies are being conducted to improve the immunogenicity of subunit vaccines by creating nanoparticles using fusion partners. It has been confirmed that S-VP8* nanoparticles using norovirus S protein can effectively prevent a viral infection after immunization in mice with three doses [72,73]. There is another study using the P domain of norovirus VP1 as another VP8* nanoparticle [74]. P-VP8* nanoparticles of P[8], P[4], and P[6] serotypes were inoculated in mice three times and the antibody response to VP8* and each serotype of the virus was measured [74]. After P[8], P[4], and P[6] serotypes of P-VP8* were inoculated with a monomer, the cross-reactivity between each serum type and serotypes P[8] and P[4] was higher than that of P[6] [74]. Additionally, a trivalent vaccine consisting of a 1:1:1 ratio of P[8], P[4], and P[6] serotypes of P-VP8* nanoparticles induced high levels of neutralizing antibody responses to the serotypes of rotavirus included in the vaccine injected in mice [74].

Previous studies showed immunogenicity to the rotavirus VP8* nanoparticle, however, there was no increase in immunogenicity when compared to the VP8* recombinant subunit vaccine. This study presented

the results of VP8* nanoparticle expression and immunogenicity that were compared to the immunogenicity of the recombinant subunit vaccine. In this study, VP8* nanoparticles were expressed using encapsulin, a bacterial protein, to make an effective VP8* vaccine. Purified encapsulin conjugated VP8* (ENC-VP8*) was solubilized in all three serotypes and appeared to be 53 kDa in size (Fig. 4). The nanoparticle size of the encapsulin of *Thermotoga Maritima,* MSB8 strain, is approximately 24 nm [75]. The sizes of the three serotypes of ENC-VP8* nanoparticles, being 24 nm, were confirmed using TEM, which is similar to the size of the nanoparticle *Thermotoga Maritima* MSB8 encapsulin (Fig. 6). The VP8* of P[8], P[4], and P[6] rotavirus is a strong combination of histo-blood group antigens mainly with Led H type 1 [76-79]. We confirmed the ability of ENC-VP8* and P2-VP8* to bind to Led H type 1 showing that ENC-VP8* binds stronger than P2-VP8* (Fig. 7). Additionally, the nanoparticle is displayed outside VP8* and is associated with the binding of ENC-VP8* and HBGA (Fig. 7), meaning that the nanoparticle can effectively expose the antigens when used as a vaccine. An ENC-VP8* nanoparticle strongly binds to Led H type 1 because the VP8* protein forms a dimer form that binds to HBGA using a fusion partner, which improves its binding ability [79]. ENC-VP8* nanoparticle exhibits stronger binding capabilities than the free form of P2-VP8* because they form a complex where antigens are repeatedly labeled, which has the potential to induce antibodies that inhibit virus-receptor binding more effectively [80].

Encapsulin-based nanoparticle expose antigens repeatedly on the surface, making them easily recognized by immune cells such as dendritic cells and

macrophages [53,81]. It can effectively induce an antibody response to an antigen labeled with this mechanism. It is confirmed that the antibody against M2e is effectively increased by expressing encapsulating-based nanoparticle labeling M2e of influenza [53]. This study explored the antibody response of ENC-VP8* compared to the recombinant subunit vaccine after inoculation with the mouse. First, the specific antibody response for each serotype was measured by taking advantage of the low similarity and different structure of each VP8* serum type [35]. The results showed that the viral infection can be effectively suppressed by inhibiting the binding of VP8* and Led H type 1 after inoculating the VP8* vaccine [77,82,83]. Additionally, the results showed that the induced antibody can effectively neutralize the rotavirus.

First, the antibody response was compared to the VP8* vaccine candidate of the G1P[8] serotype, the most common rotavirus [9,10]. To compare immunogenicity with ENC-G1P[8]VP8*, the most developed P2-G1P[8]VP8* antigen among the subunit vaccines was used [84]. ENC-G1P[8]VP8* or P2-G1P[8]VP8* were inoculated into the mouse at a minimum concentration of 10 μg, which was effective in previous studies [85]. Additionally, 1 μg and 5 μg of ENC-G1P[8]VP8* were inoculated respectively to compare antibody responses. The G1P[8] VP8* specific antibody response induced after inoculation of the G1P[8]VP8* monovalent vaccine showed that ENC-G1P[8]VP8* was higher when inoculated with the same amount of antigen (each 10 μg). Additionally, high antibody response was also induced when inoculated with ENC-G1P[8]VP8* (1 μg, 5 μg) than that of P2-G1P[8]VP8* (Table 4 and Fig. 8). The high dose of

ENC-G1P[8]VP8* was inoculated only twice, whereby the antibody response was higher than that of P2-G1P[8]VP8* (Table 4). HBGA blocking and PRNT assays were performed to determine whether the G1P[8]VP8* specific antibody response can prevent a viral infection. The ability to inhibit the binding of VP8* to a Led H type1 cell receptor was proportional to the extent to which VP8*-specific antibodies were induced (Fig. 16). ENC-G1P[8]VP8* inoculation groups showed higher binding inhibition ability than that of P2-G1P[8]VP8*, and the BD_{50} titer of mid and high doses of ENC-G1P[8]VP8* were 4-folds higher than that of P2-G1P[8]VP8* (Table 8.). When the neutralizing antibody response was confirmed in the serum, ENC-G1P[8]VP8* levels were approximately 5-fold higher than that of P2-G1P[8]VP8* (Table 12). As a result, it was confirmed that ENC-G1P[8]VP8* showed a higher antibody response compared to P2-G1P[8]VP8*. Particularly, 1 μg of ENC-VP8* showed a higher neutralizing antibody reaction than 10 μg of P2-G1P[8]VP8* (Table 12.).

Inoculation of 1 μg of the ENC-G1P[8]VP8* vaccine showed a higher neutralization antibody value than the recombinant subunit vaccine. G2P[4]VP8* and G2P[6]VP8* vaccines were inoculated with 0.5 μg, 2 μg, or 8 μg of ENC-G2P[4]VP8* and ENC-G2P[6]VP8* and 8 μg of P2-G2P[4]VP8* and P2-G2P[6]VP8* as positive controls. In G2P[4]VP8* monovalent vaccines, all three groups inoculated with ENC-G2P[4]VP8* induced higher G2P[4]VP8* specific antibody responses than those of P2-G2P[4]VP8* (Table 5 and Fig. 10). HBGA blocking assay results showed that ENC-G2P[4]VP8* exhibited higher binding inhibition ability than

P2-G2P[4]VP8*. After the final vaccination, a high dose of ENC-G2P[4]VP8* showed more than 6-fold higher BD_{50} titer than P2-G2P[4]VP8* (Table 9 and Fig. 17). Additionally, when the neutralizing antibody reaction was confirmed, ENC-G2P[4]VP8* was higher than P2-G2P[4]VP8* (Table 13 and Fig. 21). When inoculated with the G2P[6]VP8* unit price vaccine, ENC-G2P[6]VP8* (high dose, 8 μg) induced G2P8*-specific antibodies that were more than twice as high as P2-G2P[6]VP8* (high dose, 8 μg) (Table 6). The ability to inhibit G2P[6]VP8*-Led H type 1 binding was also shown to be high in ENC-G2P[6]VP8* and 3-fold higher in BD_{50} titer (Table 10). Neutralizing antibody reactions induced by ENC-G2P[6]VP8* were 2-fold higher than P2-G2P[6]VP8*, showing a similar pattern to that of VP8* specific antibody reactions (Table 14). These results showed that P[4] and P[6] serotype monovalent ENC-VP8* induced higher antibody response than P2-VP8* and 0.5 μg of ENC-VP8* inoculation induced neutralizing antibodies against viral infections in mice.

To confirm the efficacy of the rotavirus VP8* trivalent vaccine, an antigen was mixed and inoculated at a ratio of 1:1:1. A total of 1.5 μg, 6 μg and 24 μg of ENC-VP8* were inoculated at the same rate based on 0.5 μg of each P[8], P[4], and P[6] serotype ENC-VP8*, the minimum concentration that was effective in the previous experiment. A total of 24 μg of P2-VP8* was inoculated with P[8], P[4], and P[6] serotype antigens at a ratio of 1:1:1. P[8] and P[4] VP8* specific antibody responses were more than 1.5-fold higher, and P[6] VP8* showed more than 5-fold higher antibody responses (Table 7). Additionally, the ability to inhibit receptor

binding is more than 3-fold greater than that of trivalent ENC-VP8* for P[8] VP8* and P[6] VP8*, and in P[4] VP8*, it was more than 6-fold greater than that of trivalent P2-VP8* (Table 11). As a result of the PRNT assay, trivalent ENC-VP8* inhibits infection of the three virus serotypes more effectively than trivalent P2-VP8* (Table 15). As a result, it was confirmed that when P[8], P[4], and P[6] VP8* were inoculated with a trivalent vaccine at the same ratio, a uniform immune response was induced for each serotype. It was found that the trivalent ENC-VP8* showed higher vaccine efficacy than that of the trivalent P2-VP8*.

Encapsulin-based nanoparticles are easily recognized by immune cells and effectively activate the innate immune response [48,56]. Previous studies showed that the immune response occurred effectively after vaccination and improved the T helper 1 cell (Th1) response [56]. Through the ELISPOT assay, it was found that monovalent and trivalent ENC-VP8* vaccines induced both IFN-γ and IL-4 responses, however, P2-VP8* induced mainly an IL-4 response (Fig. 24-27). This shows that ENC-VP8* induces cytotoxic T-cell response more effectively, meaning that virus-infected cells can be more effectively removed.

In conclusion, this study using encapsulin as a fusion partner, nanoparticles displayed P[8], P[4], and P[6] VP8* were effectively expressed using *E.coli*. An evaluation method was established to measure antibody response and T cell response to evaluate the efficacy of rotavirus vaccine. This evaluation method compared the efficacy of encapsulin-based nanoparticles and recombinant protein-based P2-VP8* of P[8], P[4], and P[6] serotypes, showing that ENC-VP8* induces a better antibody response.

Additionally, it was shown that a viral infection can be effectively suppressed through this antibody response. Therefore, we have shown that ENC-VP8* is an effective vaccine candidate to prevent P[8], P[4], and P[6] serotypes of rotavirus infection. In order to commercialize the rotavirus nanoparticle vaccine after this study, it is necessary to establish a rotavirus infection model and confirm that the rotavirus replication is effectively suppressed in animals after vaccination [38]. Since then, it is considered necessary to conduct pre-clinical tests to confirm the toxicity and physiological safety of vaccines in rodents and non-rodents [27]. Finally, based on the results of these studies, antigens and supplements that can be effective in clinical trials should be established. [38].

논문개요

로타바이러스 A 는 사람에게 감염되어 장염을 일으키는 바이러스로 P[8] ,P[4], P[6] 세가지 혈청형의 바이러스가 전세계적으로 유행하고 있다. 매년 146,000 ~ 215,000 명의 사람들이 로타바이러스 감염으로 사망한다고 보고되고 있으며 이를 예방하기 위해서 경구 생백신 제형의 RotaTeq® (Merck)와 Rotarix® (GlaxoSmithKline, GSK)가 개발되어 전 세계적으로 사용되고 있다. 하지만 일부 국가에서 생백신의 효능이 떨어지고 부작용이 나타나는 사례가 있으며 이 때문에 안전하고 효과적인 새로운 로타바이러스 백신 개발이 필요하다.

로타바이러스 A의 VP8은 로타바이러스 감염을 예방하기위한 중화항체가 결합하는 단백질로 로타바이러스 감염을 예방하기 위한 백신 후보 물질이다. 하지만 재조합 단백질 제형의 백신을 접종할 경우 낮은 면역원성을 보이는 한계가 있으며 이를 극복하기 위해 면역보조제를 이용하는 등 면역원성을 증진시킬 방법이 필요하다. 또한 P[8] ,P[4], P[6]간의 낮은 서열 유사성으로 인해 3가 백신으로 접종할 필요가 있다. 본 연구에서는 로타바이러스 VP8의 면역원성을 증진시키기 위해 박테리아 단백질인 엔켑슐린을 이용하여 나노입자 형태로 만들어 주었다.

P[8] ,P[4], P[6] 세 가지 혈청형의 ENC-VP8*이 나노입자 형태를 이루는 것을 투사전자현미경을 이용해 확인하였으며 생물학적 특성을 HBGA binding assay를 이용하여 분석하였다. 이후 단가 또는 3가의 VP8* 백신을 마우스에 3번 접종하여 면역반응을 확인하였고 ELISA 결과, ENC-VP8*이 P2-VP8*보다 높은 결합항체 반응을 유도한 것을 보았다. 또한 PRNT assay와 HBGA blocking assay를 이용하여 중화항체 반응을 보았을 때도 ENC-VP8*이 더 높은 항체 반응을 유도하였다. 본 연구를 통하여

ENC-VP8*이 나노입자를 이루는 것을 확인하였으며 HBGA에 결합하는 것 또한 확인하였다. 또한 로타바이러스 백신의 효능을 평가하기 위한 항체 반응과 T 세포 반응을 측정하는 평가법을 확립하였으며 이를 이용해 VP8* 나노입자 백신이 재조합 단백질 백신보다 효과적으로 면역반응을 유도한 것으로 로타바이러스 예방을 위한 효과적인 백신 후보물질임을 확인하였다.

Reference

1. Dennehy PH., 2015. Rotavirus infection: A disease of the past? Infect Dis Clin North Am, 29(4), pp. 617-635.

2. Leung AK, Kellner JD, Davies HD., 2005. Rotavirus gastroenteritis. Adv Ther, 22(5) pp. 476-487.

3. Steele JC,Jr. 1999. Rotavirus. Clin Lab Med,19(3), pp. 691-703.

4. Kirkwood CD. 2010. Genetic and antigenic diversity of human rotaviruses: Potential impact on vaccination programs. J Infect Dis. pp. 202 Suppl:43.

5. Bishop R. Discovery of rotavirus: Implications for child health. J Gastroenterol Hepatol. 2009;24 Suppl 3:81.

6. Jayaram H, Estes MK, Prasad BV. 2004. Emerging themes in rotavirus cell entry, genome organization, transcription and replication. Virus Res, 101(1), pp. 67-81.

7. GBD Diarrhoeal Diseases Collaborators. 2017. Estimates of global, regional, and national morbidity, mortality, and aetiologies of diarrhoeal diseases: A systematic analysis for the global burden of disease study 2015. Lancet Infect Dis, 17(9), pp. 909-948.

8. Tate JE, Burton AH, Boschi-Pinto C, Parashar UD, 2016. World Health Organization-Coordinated Global Rotavirus Surveillance Network. Global, regional, and national estimates of rotavirus mortality in children <5 years of age, 2000-2013. Clin Infect Dis. pp. 62 Suppl 2:S96-S105.

9. Heylen E, Zeller M, Ciarlet M, et al. 2016. Human P[6] rotaviruses from sub-saharan africa and southeast asia are closely related to those of human P[4] and P[8] rotaviruses circulating worldwide. J Infect Dis, 214(7),

pp. 1039-1049.

10. Santos N, Hoshino Y. 2005. Global distribution of rotavirus serotypes/genotypes and its implication for the development and implementation of an effective rotavirus vaccine. Rev Med Virol, 15(1), pp. 29-56.

11. Kim MJ, Jeong HS, Kim SG, et al. 2014. Diversity of rotavirus strain circulated in gwangju, republic of korea. Osong Public Health Res Perspect, 5(6), pp. 364-369.

12. WHO. 2010. Meeting of the strategic advisory group of experts on immunization, october 2009 - conclusions and recommendations. Wkly Epidemiol Rec, 84(50), pp. 517-532.

13. WHO. 2013. Rotavirus vaccines. WHO position paper - january 2013. Wkly Epidemiol Rec, 88(5), pp. 49-64.

14. Burnett E, Parashar U, Tate J. 2018. Rotavirus vaccines: Effectiveness, safety, and future directions. Paediatr Drugs, 20(3) pp. 223-233.

15. Vesikari T, Matson DO, Dennehy P, et al. 2006. Safety and efficacy of a pentavalent human-bovine (WC3) reassortant rotavirus vaccine. N Engl J Med, 354(1), pp. 23-33.

16. O'Ryan M, Linhares AC. 2009. Update on rotarix: An oral human rotavirus vaccine. Expert Rev Vaccines, 8(12), pp. 1627-1641.

17. Santos VS, Marques DP, Martins-Filho PR, Cuevas LE, Gurgel RQ. 2017. Effectiveness of rotavirus vaccines against rotavirus infection and hospitalization in latin america: Systematic review and meta-analysis. Infect Dis Poverty, 5(1), pp. 83.

18. Naylor C, Lu M, Haque R, et al. 2015. Environmental enteropathy, oral vaccine failure and growth faltering in infants in bangladesh. EBioMedicine, 2(11), pp. 1759-1766.

19. Parker EPK, Praharaj I, Zekavati A, et al. 2018. Influence of the intestinal microbiota on the immunogenicity of oral rotavirus vaccine given to infants in south india. Vaccine, 36(2), pp. 264-272.

20. Velasquez DE, Parashar U, Jiang B. 2018. Decreased performance of live attenuated, oral rotavirus vaccines in low-income settings: Causes and contributing factors. Expert Rev Vaccines, 17(2), pp. 145-161.

21. Taniuchi M, Platts-Mills JA, Begum S, Uddin MJ, Sobuz SU, Liu J, Kirkpatrick BD, Colgate ER, Carmolli MP, Dickson DM, Nayak U, Haque R, Petri WA Jr, Houpt ER. 2016. Impact of enterovirus and other enteric pathogens on oral polio and rotavirus vaccine performance in Bangladeshi infants. Vaccine, 34(27) pp. 3068-3075.

22. Richie EE, Punjabi NH, Sidharta YY, et al. 2000. Efficacy trial of single-dose live oral cholera vaccine CVD 103-HgR in north jakarta, indonesia, a cholera-endemic area. Vaccine, 18(22), pp. 2399-2410.

23. Patriarca PA, Wright PF, John TJ. 1991. Factors affecting the immunogenicity of oral poliovirus vaccine in developing countries: Review. Rev Infect Dis, 13(5), pp. 926-939.

24. Glass RI, Parashar UD. 2014. Rotavirus vaccines--balancing intussusception risks and health benefits. N Engl J Med, 370(6), pp. 568-570.

25. Kirkwood CD, Ma LF, Carey ME, Steele AD. 2019. The rotavirus vaccine development pipeline. Vaccine, 37(50), pp. 7328-7335.

26. Li T, Lin H, Zhang Y, et al. 2014. Improved characteristics and protective efficacy in an animal model of E. coli-derived recombinant double-layered rotavirus virus-like particles. Vaccine, 32(17), pp. 1921-1931.

27. Groome MJ, Koen A, Fix A, et al. 2017. Safety and immunogenicity of a parenteral P2-VP8-P[8] subunit rotavirus vaccine in toddlers and infants in south africa: A randomised, double-blind, placebo-controlled trial. Lancet Infect Dis, 17(8), pp. 843-853.

28. Suzuki H. 2019. Rotavirus replication: Gaps of knowledge on virus entry and morphogenesis. Tohoku J Exp Med, 248(4), pp. 285-296.

29. Rakau KG, Nyaga MM, Gededzha MP, et al. 2021. Genetic characterization of G12P[6] and G12P[8] rotavirus strains collected in six african countries between 2010 and 2014. BMC Infect Dis, 21(1), pp. 107.

30. Taraporewala ZF, Patton JT. 2004. Nonstructural proteins involved in genome packaging and replication of rotaviruses and other members of the reoviridae. Virus Res, 101(1), pp. 57-66.

31. Bishop RF. 1996. Natural history of human rotavirus infection. Arch Virol Suppl, 12, pp. 119-128.

32. Pesavento JB, Crawford SE, Estes MK, Prasad BV. 2006. Rotavirus proteins: Structure and assembly. Curr Top Microbiol Immunol, 309, pp. 189-219.

33. Patton JT. 2012. Rotavirus diversity and evolution in the post-vaccine world. Discov Med, 13(68). pp. 85-97.

34. Arias CF, Isa P, Guerrero CA, et al. 2002. Molecular biology of rotavirus cell entry. Arch Med Res, 33(4). pp. 356-361.

35. Wen X, Cao D, Jones RW, Li J, Szu S, Hoshino Y. 2012. Construction

and characterization of human rotavirus recombinant VP8* subunit parenteral vaccine candidates. Vaccine, 30(43), pp. 6121-6126.

36. Xue M, Yu L, Che Y, et al. 2015. Characterization and protective efficacy in an animal model of a novel truncated rotavirus VP8 subunit parenteral vaccine candidate. Vaccine, 33(22), pp. 2606-2613.

37. Wen X, Cao D, Jones RW, Hoshino Y, Yuan L. 2015. Tandem truncated rotavirus VP8* subunit protein with T cell epitope as non-replicating parenteral vaccine is highly immunogenic. Hum Vaccin Immunother, 11(10), pp. 2483-2489.

38. Lakatos K, McAdams D, White JA, Chen D. 2020. Formulation and preclinical studies with a trivalent rotavirus P2-VP8 subunit vaccine. Hum Vaccin Immunother, 16(8), pp. 1957-1968.

39. Nooraei S, Bahrulolum H, Hoseini ZS, et al. 2021. Virus-like particles: Preparation, immunogenicity and their roles as nanovaccines and drug nanocarriers. J Nanobiotechnology, 19(1), pp. 59-7.

40. Grego EA, Siddoway AC, Uz M, et al. 2021. Polymeric nanoparticle-based vaccine adjuvants and delivery vehicles. Curr Top Microbiol Immunol, 433, pp. 29-76.

41. Plevka P, Tars K, Liljas L. 2009. Structure and stability of icosahedral particles of a covalent coat protein dimer of bacteriophage MS2. Protein Sci, 18(8), pp. 1653-1661.

42. Wynne SA, Crowther RA, Leslie AG. 1999. The crystal structure of the human hepatitis B virus capsid. Mol Cell, 3(6), pp. 771-780.

43. Tan M, Jiang X. 2019. Norovirus capsid protein-derived nanoparticles and polymers as versatile platforms for antigen presentation and vaccine

development. Pharmaceutics, 11(9), pp. 472.

44. Gabashvili AN, Chmelyuk NS, Efremova MV, Malinovskaya JA, Semkina AS, Abakumov MA. 2020. Encapsulins-bacterial protein nanocompartments: Structure, properties, and application. Biomolecules, 10(6), pp. 966.

45. Bachmann MF, Jennings GT. 2010. Vaccine delivery: A matter of size, geometry, kinetics and molecular patterns. Nat Rev Immunol, 10(11), pp. 787-796.

46. Malachowski T, Hassel A. 2020. Engineering nanoparticles to overcome immunological barriers for enhanced drug delivery. Engineered Regeneration, 1, pp. 35-50.

47. Boraschi D, Italiani P, Palomba R, Decuzzi P, Duschl A, Fadeel B, Moghimi SM. 2017. Nanoparticles and innate immunity: new perspectives on host defence. Semin Immunol, 34, pp. 33-51.

48. Szeto GL, Lavik EB. 2016. Materials design at the interface of nanoparticles and innate immunity. J Mater Chem B, 4(9), pp. 1610-1618.

49. Jones JA, Giessen TW. 2021. Advances in encapsulin nanocompartment biology and engineering. Biotechnol Bioeng, 118(1), pp. 491-505.

50. Sutter M, Boehringer D, Gutmann S, et al. 2008. Structural basis of enzyme encapsulation into a bacterial nanocompartment. Nat Struct Mol Biol, 15(9), pp. 939-947.

51. Van de Steen A, Khalife R, Colant N, et al. 2021. Bioengineering bacterial encapsulin nanocompartments as targeted drug delivery system. Synth Syst Biotechnol, 6(3), pp. 231-241.

52. Michel-Souzy S, Hamelmann NM, Zarzuela-Pura S, Paulusse JMJ, Cornelissen JJLM. 2021. Introduction of surface loops as a tool for encapsulin functionalization. Biomacromolecules, 22(12), pp. 5234-5242.

53. Lagoutte P, Mignon C, Stadthagen G, et al. 2018. Simultaneous surface display and cargo loading of encapsulin nanocompartments and their use for rational vaccine design. Vaccine, 36(25), pp. 3622-3628.

54. Kar U, Khaleeq S, Garg P, et al. 2022. Comparative immunogenicity of bacterially expressed soluble trimers and nanoparticle displayed influenza hemagglutinin stem immunogens. Front Immunol, 13, pp. 890622.

55. Kanekiyo M, Bu W, Joyce MG, et al. 2015. Rational design of an epstein-barr virus vaccine targeting the receptor-binding site. Cell, 162(5), pp. 1090-1100.

56. Choi B, Moon H, Hong SJ, et al. 2016. Effective delivery of antigen-encapsulin nanoparticle fusions to dendritic cells leads to antigen-specific cytotoxic T cell activation and tumor rejection. ACS Nano, 10(8), pp. 7339-7350.

57. Cappelli L, Cinelli P, Giusti F, et al. Self-assembling protein nanoparticles and virus like particles correctly display β-barrel from meningococcal factor H-binding protein through genetic fusion. PLoS One. 2022;17(9):e0273322.

58. Wen X, Wen K, Cao D, et al. 2014. Inclusion of a universal tetanus toxoid CD4(+) T cell epitope P2 significantly enhanced the immunogenicity of recombinant rotavirus ΔVP8* subunit parenteral vaccines. Vaccine, 32(35), pp. 4420-4427.

59. Choi D, Jong HG, inventors 2021. RECOMBINANT EXPRESSION

VECTOR FOR PRODUCTION OF ENCAPSULIN-BASED VACCINE AND METHOD FOR MANUFACTURING THE SAME. patent 10-2264535-0000.

60. InThera, Inc. 2022. Pre-clinical study of Non-replicating Protein nanoparticle-based Rotavirus Vaccine. RIGHT Fund Milestone Report. RF-TAA-2021-V02

61. Lim J, Cheong Y, Kim YS, et al. 2021. RNA-dependent assembly of chimeric antigen nanoparticles as an efficient H5N1 pre-pandemic vaccine platform. Nanomedicine, 37, pp. 102438.

62. Yang SW, Jang YH, Kwon SB, et al. 2018. Harnessing an RNA-mediated chaperone for the assembly of influenza hemagglutinin in an immunologically relevant conformation. FASEB J, 32(5), pp. 2658-2675.

63. Huang P, Farkas T, Marionneau S, et al. 2003. Noroviruses bind to human ABO, lewis, and secretor histo-blood group antigens: Identification of 4 distinct strain-specific patterns. J Infect Dis, 188(1), pp. 19-31.

64. Quan FS, Compans RW, Nguyen HH, Kang SM. 2008. Induction of heterosubtypic immunity to influenza virus by intranasal immunization. J Virol, 82(3), pp. 1350-1359.

65. Reeck A, Kavanagh O, Estes MK, et al. 2010. Serological correlate of protection against norovirus-induced gastroenteritis. J Infect Dis, 202(8), pp. 1212-1218.

66. Knowlton DR, Spector DM, Ward RL. 1991. Development of an improved method for measuring neutralizing antibody to rotavirus. J Virol Methods, 33(1-2), pp. 127-134.

67. Quan FS, Huang C, Compans RW, Kang SM. 2007. Virus-like particle vaccine induces protective immunity against homologous and heterologous

strains of influenza virus. J Virol, 81(7), pp. 3514-3524.

68. Velasquez DE, Jiang B. 2019. Evolution of P[8], P[4], and P[6] VP8* genes of human rotaviruses globally reported during 1974 and 2017: Possible implications for rotavirus vaccines in development. Hum Vaccin Immunother, 15(12), pp. 3003-3008.

69. Vila-Vicent S, Gozalbo-Rovira R, Rubio-Del-Campo A, et al. 2020. Sero-epidemiological study of the rotavirus VP8* protein from different P genotypes in valencia, spain. Sci Rep, 10(1), pp. 7753-x.

70. Hong MS, Kaur K, Sawant N, Joshi SB, Volkin DB, Braatz RD. 2021. Crystallization of a nonreplicating rotavirus vaccine candidate. Biotechnol Bioeng, 118(4), pp. 1750-1756.

71. Jia L, Li T, Ge S. 2017. Research progress in rotavirus VP4 subunit vaccine. Sheng Wu Gong Cheng Xue Bao, 33(7), pp. 1075-1084.

72. Xia M, Huang P, Sun C, et al. 2018. Bioengineered norovirus S(60) nanoparticles as a multifunctional vaccine platform. ACS Nano, 12(11), pp. 10665-10682.

73. Xia M, Huang P, Jiang X, Tan M. 2019. Immune response and protective efficacy of the S particle presented rotavirus VP8* vaccine in mice. Vaccine, 37(30), pp. 4103-4110.

74. Xia M, Huang P, Jiang X, Tan M. 2021. A nanoparticle-based trivalent vaccine targeting the glycan binding VP8* domains of rotaviruses. Viruses, 13(1), pp. 72.

75. Lagoutte P, Mignon C, Stadthagen G, et al. 2018. Simultaneous surface display and cargo loading of encapsulin nanocompartments and their use for rational vaccine design. Vaccine, 36(25), pp. 3622-3628.

76. Hu L, Sankaran B, Laucirica DR, et al. 2018. Glycan recognition in globally dominant human rotaviruses. Nat Commun, 9(1), pp. 2631-2634.

77. Haselhorst T, Fleming FE, Dyason JC, et al. 2009. Sialic acid dependence in rotavirus host cell invasion. Nat Chem Biol, 5(2), pp. 91-93.

78. Sun X, Guo N, Li D, et al. 2016. Binding specificity of P[8] VP8* proteins of rotavirus vaccine strains with histo-blood group antigens. Virology, 495, pp. 129-135.

79. Huang P, Xia M, Tan M, et al. 2012. Spike protein VP8* of human rotavirus recognizes histo-blood group antigens in a type-specific manner. J Virol, 86(9), pp. 4833-4843.

80. Tan M, Huang P, Xia M, et al. 2011. Norovirus P particle, a novel platform for vaccine development and antibody production. J Virol, 85(2), pp. 753-764.

81. Choi B, Moon H, Hong SJ, et al. 2016. Effective delivery of antigen-encapsulin nanoparticle fusions to dendritic cells leads to antigen-specific cytotoxic T cell activation and tumor rejection. ACS Nano, 10(8), pp. 7339-7350.

82. Cantelli CP, Velloso AJ, Assis RMS, et al. 2020. Rotavirus A shedding and HBGA host genetic susceptibility in a birth community-cohort, rio de janeiro, brazil, 2014-2018. Sci Rep, (1), pp. 6965-0.

83. Hu L, Crawford SE, Czako R, et al. 2012. Cell attachment protein VP8* of a human rotavirus specifically interacts with A-type histo-blood group antigen. Nature, 485(7397), pp. 256-259.

84. Groome MJ, Fairlie L, Morrison J, et al. 2020. Safety and immunogenicity of a parenteral trivalent P2-VP8 subunit rotavirus vaccine:

A multisite, randomised, double-blind, placebo-controlled trial. Lancet Infect Dis, 20(7), pp. 851-863.

85. Fix AD, Harro C, McNeal M, et al. 2015. Safety and immunogenicity of a parenterally administered rotavirus VP8 subunit vaccine in healthy adults. Vaccine, 33(31), pp. 3766-3772.

감사의 글

학부생 때 졸업하면 연구를 해보고 싶다는 마음으로 실험실 생활을 시작하였고, 하나를 파면 끝까지 파보는 성격에 기왕이면 박사까지 해봐야지 라는 마음으로 시작한 대학원 생활이 2015년부터 시작해 벌써 8년의 시간이 흘렀네요. 짧지 않은 시간을 쏟으면서 값진 것들을 배울 수 있었고 비록 일이 잘 풀리지 않을 때는 회의감이 들기도 했지만 여전히 연구하는 것이 좋고 뒤 돌아 보며 쌓아둔 것들을 보니 이 시간이 헛되진 않았던 것 같습니다. 학위 과정 중에 사랑하는 사람을 만나 가정을 이루고 소중한 자녀 까지 얻었으니 뒤 돌아 보니 너무 감사한 시간이었고 또 여러 시행착오를 치르면서 막막했던 이 시간이 끝맺음을 맺으니 너무 뿌듯한 마음입니다.

학위를 마치며 가장 먼저 박사학위 기간 동안 잘 이끌어 주신 송재민 교수님께 감사의 말씀 올리고 싶습니다. 타 학교에 대학원 진학하여 학위를 마치는 것이 쉽지는 않았는데 교수님께서 잘 이끌어주신 덕분에 순조롭게 졸업까지 잘 미칠 수 있었던 것 같습니다. 또 교수님께서 힘써주신 덕분에 다양한 연구를 진행 할 수 있었고 함께 고민해주시고 지도해 주신 덕분에 이 모든 시간이이 앞으로의 발걸음에 좋은 밑거름이 되었습니다. 항상 건강하시고 하시는 일에 좋은 결과 있기를 바랍니다.

학위논문 심사를 맡아 고견을 보태주신 심사위원 분들께도 감사의 말씀 올립니다. 심사위원장을 맡아 쭉 이끌어주신 고병준 교수님, 심사위원으로 논문이 완성되기 까지 의견을 제시해주신 임동현 교수님, 먼 곳에서 발걸음 해주셔서 많은 도움주신 가톨릭대학교 서상욱 교수님, 국민대학교 강태현 교수님께 감사 인사 올립니다. 바쁘신 와중에도 시간을 내어주시고 심사 때 많은 고견 제시해주신 덕분에 학위논문이 풍성하게 완성될 수 있었습니다.

다음으로 8년 동안 동고동락한 실험실 후배들에게도 감사의 인사 드립니

다. 졸업으로 먼저 학교를 떠난 재인이와 현영이 이제 다음으로 졸업을 앞둔 소화와 예은이 그리고 다빈누나 까지 모두에게 감사합니다. 실험실 내에서 자잘한 부분들 챙겨주고 도와주어서 여기까지 잘 올 수 있었습니다. 남은 시간도 잘 부탁하고 앞으로 준비하고 하는 일 모두 잘되길 바랍니다.

그리고 언제나 제 선택을 응원해 주시고 지켜봐 주시는 어머니와 가족들에게 감사드립니다. 앞으로 더 노력하는 아들이 되도록 노력하겠습니다. 겉으로 보면 무뚝뚝함이 매력인 동생들에게도 응원해주어서 고맙다고 말하고 싶습니다. 그리고 이 모습 보면 가장 좋아하셨을 하늘로 가신 아버지께도 감사 올립니다. 아버지가 저에게 항상 자랑스러웠듯이 저도 하늘에서 보기에 자랑스러운 아들이 되도록 노력하겠습니다. 앞으로도 우리 가족 잘 사는 모습 보여드리겠습니다.

이 세상 하나뿐인 사랑하는 아내 지혜에게도 고맙다는 말 전합니다. 언제나 툴툴 거려도 잘 받아주고 매일매일 행복하게 해주어 고마워. 약속한데로 언제나 행복한 마음 느끼면서 잘 살아보자. 그리고 올해 찾아온 세상 가장 소중한 하운이도 아프지 않고 건강하게 자라주어서 고맙다는 말 전합니다.

여기에 적진 못했지만 제 삶에서 함께해준 분들께도 너무나 감사하다는 말 전해드리며 이만 마치겠습니다.